USGS
science for a changing world

Soil CO_2 Flux in the Amargosa Desert, Nevada, during El Niño 1998 and La Niña 1999

Scientific Investigations Report 2009–5061

U.S. Department of the Interior
U.S. Geological Survey

COVER: Autochambers in the Amargosa Desert.

Soil CO_2 Flux in the Amargosa Desert, Nevada, during El Niño 1998 and La Niña 1999

By Alan C. Riggs, David I. Stannard, Florentino B. Maestas, Michael R. Karlinger, and Robert G. Striegl

Scientific Investigations Report 2009–5061

U.S. Department of the Interior
U.S. Geological Survey

U.S. Department of the Interior
KEN SALAZAR, Secretary

U.S. Geological Survey
Marcia K. McNutt, Director

U.S. Geological Survey, Reston, Virginia: 2009

Suggested citation:
Riggs, A.C., Stannard, D.I., Maestas, F.B., Karlinger, M.R., and Striegl, R.G., 2009, Soil CO_2 flux in the Amargosa Desert, Nevada, during El Niño 1998 and La Niña 1999: U.S. Geological Survey Scientific Investigations Report 2009–5061, 25 p.

Contents

Figures

Tables

Conversion Factors

Multiply	By	To obtain
	Length	
centimeter (cm)	0.3937	inch (in.)
millimeter (mm)	0.03937	inch (in.)
meter (m)	3.281	foot (ft)
kilometer (km)	0.6214	mile (mi)
kilometer (km)	0.5400	mile, nautical (nmi)
	Area	
square meter (m^2)	10.76	square foot (ft^2)
square centimeter (cm^2)	0.1550	square inch (ft^2)
	Volume	
liter (L)	33.82	ounce, fluid (fl. oz)
cubic decimeter (dm^3)	0.2642	gallon (gal)
cubic centimeter (cm^3)	0.06102	cubic inch (in^3)
liter (L)	61.02	cubic inch (in^3)
	Flow rate	
meter per second (m/s)	3.281	foot per second (ft/s)
liter per second (L/s)	15.85	gallon per minute (gal/min)
kilometer per hour (km/h)	0.6214	mile per hour (mi/h)
	Mass	
gram (g)	0.03527	ounce, avoirdupois (oz)
kilogram (kg)	2.205	pound avoirdupois (lb)
	Pressure	
atmosphere, standard (atm)	101.327	kilopascal (kPa)
atmosphere, standard (atm)	1.0133	bar
atmosphere, standard (atm)	29.92	inch of mercury at 0°F (in Hg)
atmosphere, standard (atm)	14.696	pound-force per square inch (lbf/in^2)
	Density	
kilogram per cubic meter (kg/m^3)	0.06242	pound per cubic foot (lb/ft^3)
gram per cubic centimeter (g/cm^3)	62.4220	pound per cubic foot (lb/ft^3)
	Energy Flux Density	
µEinstein per square meter per second (µE/m^2 sec)	0.217	≈Watts per square meter (W/m^2)
Watts per square meter (W/m^2)	0.000088055	British thermal units per square foot per second (Btu/ft^2 sec)
Watts per square meter (W/m^2)	0.00023885	Kilocalorie per square meter per second (kcal/m^2 sec)

Temperature in degrees Celsius (°C) may be converted to degrees Fahrenheit (°F) as follows:

$$°F=(1.8\times°C)+32$$

Temperature in degrees Fahrenheit (°F) may be converted to degrees Celsius (°C) as follows:

$$°C=(°F-32)/1.8$$

Vertical coordinate information is referenced to the "North American Vertical Datum of 1988 (NAVD 88)"

Horizontal coordinate information is referenced to the "North American Datum of 1983 (NAD 83)"

Altitude, as used in this report, refers to distance above the vertical datum.

Abbreviations

CO_{2air}	Carbon dioxide derived from the atmosphere
CO_{2biol}	Carbon dioxide produced by the metabolic activities of living organisms
CO_{2gw}	Carbon dioxide exsolved from groundwater
DOY	Day of Year
ET	Evapotranspiration
PAR	Photosynthetically active radiation
/	Divided by (in mathematical expressions)
×	Times, or multiplied by
<	Less than, fewer than
≤	Less than or equal to, fewer than or equal to
>	More than, greater than
≥	More than or equal to, greater than or equal to
≈	Approximately equal to

Soil CO_2 Flux in the Amargosa Desert, Nevada, during El Niño 1998 and La Niña 1999

By Alan C. Riggs, David I. Stannard, Florentino B. Maestas, Michael R. Karlinger,[1] and Robert G. Striegl

Abstract

Mean annual soil CO_2 fluxes from normally bare mineral soil in the Amargosa Desert in southern Nevada, United States, measured with clear and opaque soil CO_2-flux chambers (autochambers) were small—<5 millimoles per square meter per day—during both El Niño 1998 and La Niña 1999. The 1998 opaque-chamber flux exceeded 1999 opaque-chamber flux by an order of magnitude, whereas the 1998 clear-chamber flux exceeded 1999 clear-chamber flux by less than a factor of two. These data suggest that above-normal soil moisture stimulated increased metabolic activity, but that much of the extra CO_2 produced was recaptured by plants. Fluxes from warm moist soil were the largest sustained fluxes measured, and their hourly pattern is consistent with enhanced soil metabolic activity at some depth in the soil and photosynthetic uptake of a substantial portion of the CO_2 released. Flux from cool moist soil was smaller than flux from warm moist soil. Flux from hot dry soil was intermediate between warm-moist and cool-moist fluxes, and clear-chamber flux was more than double the opaque-chamber flux, apparently due to a chamber artifact stemming from a thermally controlled CO_2 reservoir near the soil surface. There was no demonstrable metabolic contribution to the very small flux from cool dry soil, which was dominated by diffusive up-flux of CO_2 from the water table and temperature-controlled CO_2-reservoir up- and down-fluxes. These flux patterns suggest that transfer of CO_2 across the land surface is a complex process that is difficult to accurately measure.

Introduction

We live at a time when society is beginning to recognize the natural variability of climate over time, the potential for our activities to substantially change climate, and the large-scale disruptions that our social order is likely to experience in the face of significant climate changes, whatever their origin. Accordingly, considerable effort is being directed toward developing an enhanced understanding of the determinants of global climate and climate change. Developing a sufficiently detailed and accurate understanding of global climate so that useful predictions can be made is a difficult problem whose solution appears to be well in the future, at best. That is not to say, however, that little is known or that productive avenues of investigation are not apparent. For instance, it is widely recognized that the release into the atmosphere of natural and anthropogenically generated greenhouse gases, particularly CO_2, plays an important role in mediating earth-surface and atmospheric energy budgets (for example, Field and Raupach, 2004). Understanding the distribution of different carbon reservoirs near the earth's surface, the fluxes between them, and the feedbacks between flux and climate change is an important prerequisite to understanding global climate.

Despite concerted and continuing effort, a credible global carbon budget is yet to be developed (Field and Raupach, 2004), never mind untangling the smaller-scale subtleties associated with regional and local fluxes between carbon reservoirs. Present estimates suggest that, on a global scale, the amount of soil CO_2 released to the atmosphere is about equal to or slightly greater than terrestrial net primary productivity and about half as large as gross primary productivity (Raich and Schlesinger, 1992). Thus, an important field of investigation is the identification and quantification of the physical and biological mechanisms contributing to the flux of CO_2 between soils and the atmosphere, hereafter soil CO_2 flux or flux (the sign convention used here is that CO_2 up-fluxes are positive).

Depending on the area to be characterized, any of several methodologies may be used to measure CO_2 flux. For areas less than (<) 1 square meter (m^2), the usual method of choice is a manual soil CO_2 flux chamber—an open-bottomed chamber that is sealed to the soil surface, typically for a few minutes, while the rate of CO_2 concentration change in the air inside is measured. Given the chamber height, temperature, and barometric pressure, the flux of CO_2 between the soil and the atmosphere in the chamber can be calculated. Chambers are well suited to evaluating short-term variations in CO_2 flux from a particular location or microenvironment, but they typically have not been used to develop long-term records because of the high cost of manually placing and removing chambers, and because few of the automated soil-CO_2-flux chamber (autochamber) designs developed to date are well suited to long-term unattended operation in remote locations.

[1]U.S. Geological Survey, retired.

This report summarizes the design of an autochamber suited to long-term unattended operation and reports 2 years of hourly flux measurements made by two autochambers of the new design in the Amargosa Desert during 1998 and 1999. One of the autochambers was equipped with a clear lid and measured the flux of CO_2 across the soil surface minus the CO_2 fixed by photosynthesis. The other chamber was equipped with an opaque lid and measured the flux of CO_2 across the soil surface without the photosynthetic uptake and fixation of CO_2, which stops in darkness. Although the fluxes measured during the autochamber trial should not be taken as completely accurate (many feel that inaccuracy is a characteristic of all chamber measurements; for example, Nay and others, 1994; Healy and others, 1996; Rustad and others, 2000; Janssens and others, 2000), variations in measured fluxes are taken to be good representations of variations in the actual fluxes, except as noted. The importance of the more than (>) 33,000 flux measurements made in 1998–1999 is that their covariation with other physical variables—evapotranspiration (*ET*), soil temperature, soil heat flux, soil moisture, rainfall, and insolation—allows us to identify the processes that mediate the flux of CO_2 across the soil surface in response to varying conditions and to estimate how the flux is partitioned between the three sources of CO_2: metabolic CO_2 released by soil organisms (CO_{2biol}), CO_2 diffusing up from the water table (CO_{2gw}), and atmospheric CO_2 (CO_{2air}).

Chamber Design, Operation, and Data Collection

An autochamber is distinctly more complex than a manual chamber. The autochamber design tested in this study (fig. 1) consists of a collar that anchors the chamber in, and seals it to, the soil, clear or opaque lid with gasketed basal flange, lid support frame, hinged truss, double-acting pneumatic cylinder, sample gas intake line, sample gas return line with distribution manifold, and pressure-equilibration vent. The collar, support frame, and opaque lid are polyvinyl chloride, the clear chamber lid is polycarbonate plastic, and the truss is stainless steel tubing. Chamber installation involves (1) driving the collar, an

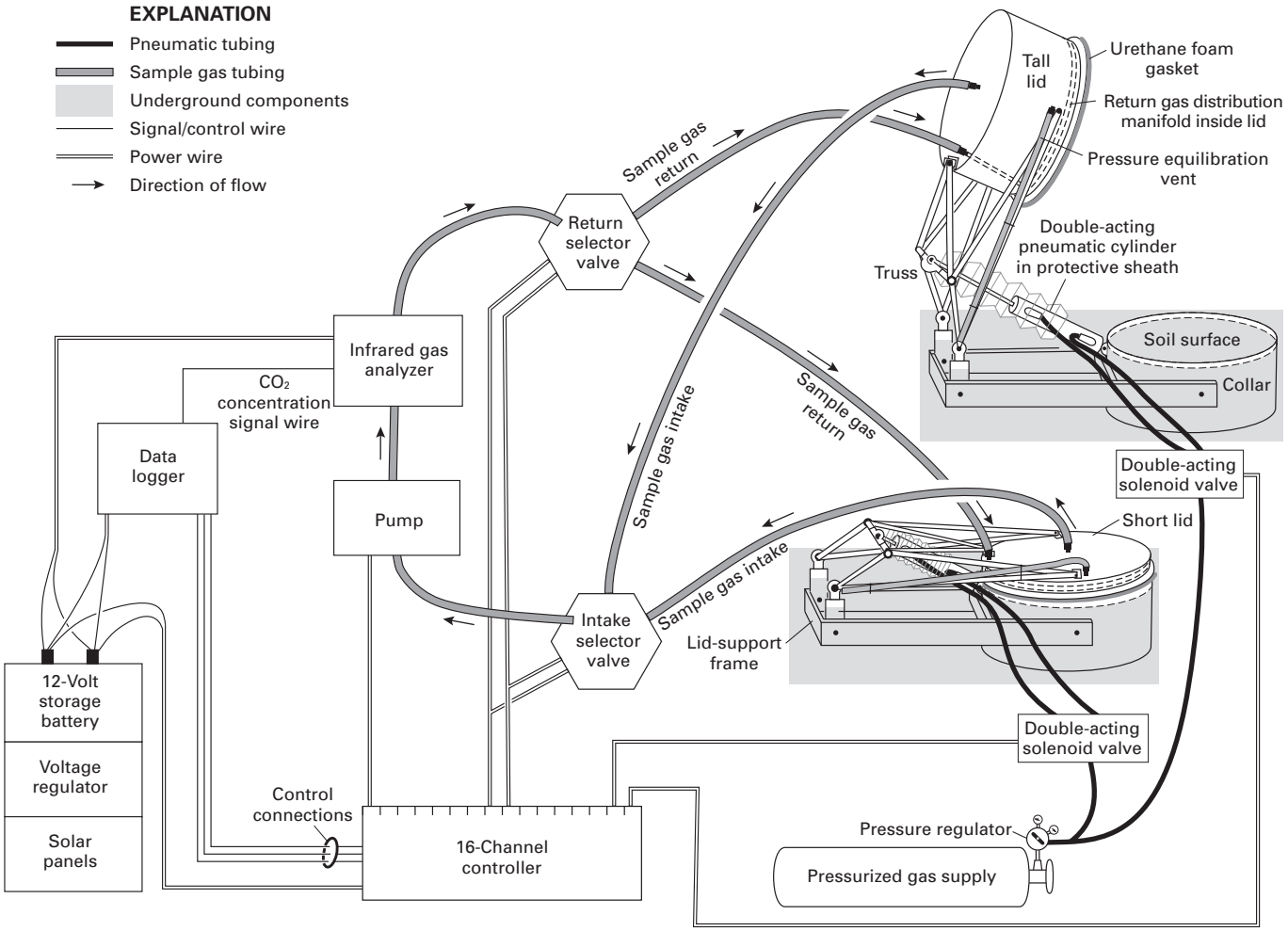

Figure 1. Schematic of the automated soil-CO_2-flux chamber system, showing chamber design (chambers are in and above the grey boxes) and the connections for power, data, control, sample gas, and pneumatic-cylinder gas.

approximately 38-centimeter (cm)-diameter (nominal 15 inches (in)) by 15-cm-long section of plastic pipe with both ends sharpened to chisel edges, into the ground until only 1–2 cm protrude above the surface; (2) excavating the soil on the perimeter of the collar away from the equator to about half the collar depth; (3) bolting the support frame to the collar below ground level and backfilling the hole; and (4) installing the truss, lid, and pneumatic cylinder and adjusting the lid so that it is centered and its gasket seals on the full circumference of the chisel-edged collar top. Except for excavating the cavity for the support frame, chamber installation minimally perturbs the soil. The lid support frame is totally buried, minimizing interference with natural air movements (fig. 1). The system shown can operate up to six chambers, though experience has shown that a maximum of four fluxes can be measured in an hour. Flux perturbations resulting from chamber installation probably damp out after a few rainfalls and thus are relatively unimportant for long-term records. In the intervals between readings, the chamber lid is held nearly upright by the extended pneumatic cylinder (figs. 1, 2). At the beginning of a measurement interval, the pneumatic cylinder contracts, pivoting the lid down to seal firmly against the collar; at the end of the measurement interval, the pneumatic cylinder extends, lifting the lid. A tall lid is used if there is tall vegetation in the chamber, and a short lid is used to increase sensitivity if vegetation is short or absent.

The CO_2-concentration measurement system consisted of a constant-volume loop of non-CO_2-absorptive BEV-A-LINE tubing that ran from the sample gas intake port in the middle of the chamber lid, through a pump and an infrared gas analyzer (IRGA), and thence back to a distribution manifold encircling the inner perimeter of the chamber lid. The setup described in this report also included two motorized selector valves, one each on the sample and return lines, so that multiple chambers (two in this study) could share a single pump, data logger, and IRGA (PP Systems WMA-2; 0–5,000 parts per million (ppm) range, ±50 ppm accuracy, 0.1 ppm precision). The data logger processed and stored the CO_2 concentrations output by the IRGA as well as the meteorological and soil data output by other instrumentation at the site (see below). The sample-gas pump, sample-gas selector valves, and solenoid valves that controlled the pneumatic cylinders were actuated by a 16-channel controller that was controlled by the data logger. Solar panels charged a deep-cycle storage battery that powered everything except the pneumatic cylinders, which were pressurized with compressed nitrogen.

Figure 3 shows the sequence of events in a 12-minute (min) flux measurement cycle. The actual flux measurement was made from minutes 6 to 10, when the lid was down. For reasons of simplicity and dependability, the only calibration procedure used, beyond the auto-zero built into the IRGA, was lid-up CO_{2air} measurement for the 2 minutes preceding and the 2 minutes following the flux measurement (minutes 4–6 and 10–12 in fig. 3). The measured CO_{2air} concentrations were assumed to be 365 parts per million volume (ppmv) and were used to scale the CO_2 values measured when the lid

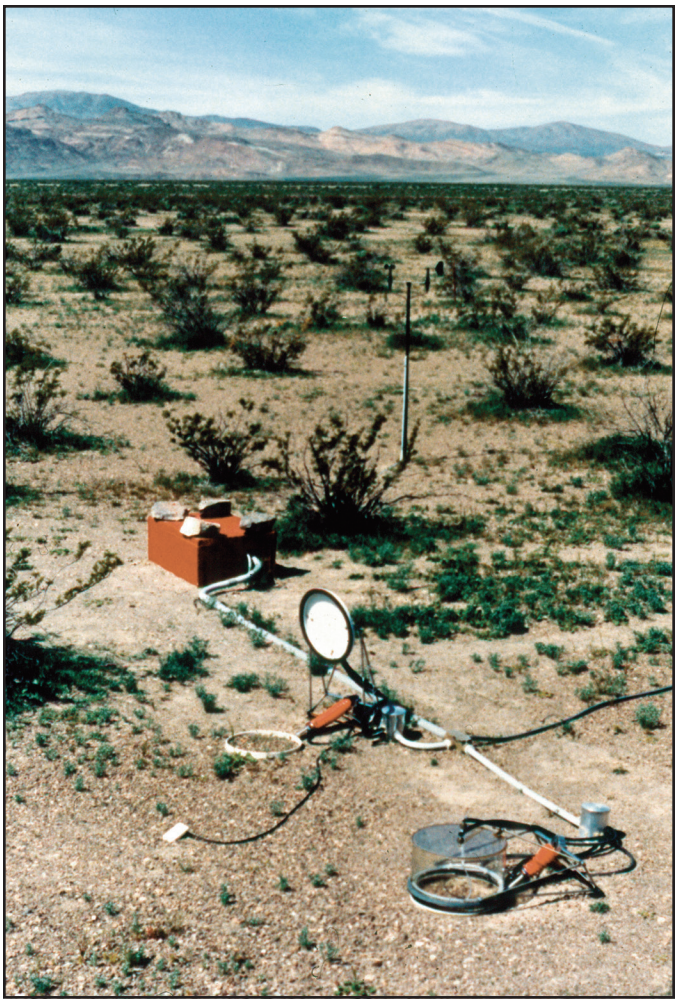

Figure 2. Autochambers in the Amargosa Desert. The tall clear chamber, lower right, is in the lid-down measuring position. The short opaque chamber, lower center, is in the lid-up park position. Both chambers had short lids during the majority of this study. The red instrument shelter, left center, contains the IRGA, data logger, pump, selector valves, 16-channel controller, deep-cycle battery, and barometer. The light gray polyvinyl chloride tubing between the instrument shelter and the chambers protects the sample-gas tubing, solenoid-valve wiring, and nitrogen tubing from damage by ultraviolet light and rodents. The pole supports the cup anemometer, wind vane, and photosynthetically active radiation sensor. The nitrogen cylinder, solar panels, and voltage regulator are not visible.

was down. Once the pump was turned on, it took at least one 2-min auto-zero cycle for lid-up CO_{2air} readings to stabilize at near-atmospheric concentration. Thus, the pump was turned on 3 minutes (minutes 1–4 in fig. 3) prior to recording CO_2 readings to avoid recording the IRGA's calibration instability after pump startup.

As originally built, the chambers had lid heights in excess of 20 cm. The large chamber volumes, coupled with the normally small CO_2 fluxes across the soil surface in the Amargosa Desert, resulted in very small CO_2-concentration changes during the 4-min measurement intervals. To increase sensitivity,

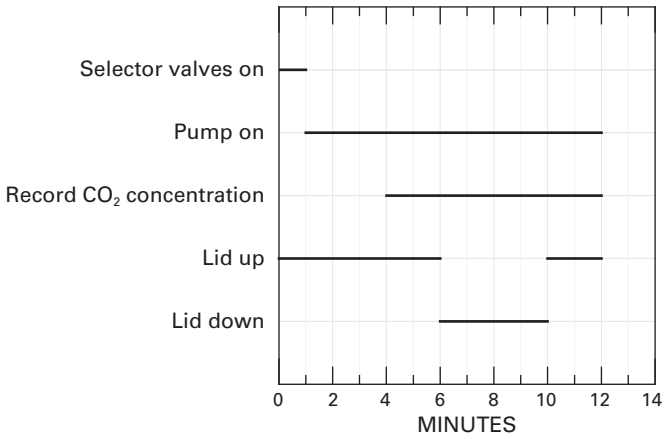

Figure 3. The sequence of events during a flux measurement.

short lids were installed on the opaque chamber (day of year (DOY) 12, 1998, fig. 2) and the clear chamber (DOY 136, 1998), giving effective heights of 5.6 cm and 5.1 cm, respectively. The switch to short lids (1) reduced the chambers' volumes, which increased CO_2 concentration changes; (2) improved circulation, with the change from a large open chamber volume with uncertain mixing of gases to a more discoid volume with radial circulation from edge to center; and (3) increased the number of chamber volumes that circulated through the sampling loop per minute by a factor of approximately 4.3. Figure 4 shows the decrease in uncertainty when a tall lid was replaced with a short one. When both chambers had short lids, measurement uncertainties were typically less than or equal to (≤) 2 millimoles per square meter per day (mmol m^{-2} d^{-1}), while flux-measurement uncertainties were roughly 4 mmol m^{-2} d^{-1} when the clear chamber had a tall lid. The offset in clear-chamber flux when the lid was switched is probably partly due to calibration differences between the two lids, but mostly due to a rapid decrease in photosynthesis as soil moisture concurrently fell below the minimum required for plant survival.

In addition to the flux chambers, site instrumentation included a cup anemometer, wind vane, tipping-bucket rain gage, soil moisture sensor (reading averaged over the top 10 cm of the soil), hygrometer/air temperature sensor, photosynthetically active radiation (*PAR*) sensor, barometer, and three soil thermistors, two at 5-cm depth and one at 10-cm depth. From minutes 4 to 12 during the flux measurement cycle, CO_2 concentrations were measured every second and stored as 10-second (s) averages. The soil moisture sensor was read once per 15-min interval, and the total number of rain gage bucket tips per 15-min interval was recorded. Battery voltage, data logger panel temperature, and all other variables were measured at 10-s intervals and 15-min averages were recorded.

Evapotranspiration (*ET*) and soil heat flux (*G*) were measured at 30-min intervals at a site approximately 50 meters (m) south of the chamber site where vegetation and soils were indistinguishable from those at the chamber site. The eddy-correlation method (Swinbank, 1951; Tanner and Greene, 1989) was used to measure *ET*. Corrections to the measured flux were made to account for density effects (Webb and others, 1980) and for the sensitivity of the hygrometer to oxygen concentration (Tanner and Greene, 1989). Multiplying *ET* in grams per square meter per second (g m^{-2} s^{-1}) by 86.4 converts it to units of millimeters per day (mm d^{-1}). Soil heat flux (W m^{-2}) was measured at two bare-soil locations using the combination method (Fuchs and Tanner, 1968; Tanner and Greene, 1989), and these measurements were averaged into a single value. Soil heat flux is a measure of the flux of heat energy into or out of the soil in response to a temperature gradient. During midday, flux of heat energy is generally downward into the soil. At night, the flux is typically upward.

The Study Site

The chambers were installed at 36°44′25″ N, 116°40′57″ W on bare mineral soil on the floor of the northwest arm of the Amargosa Desert, the next basin east of Death Valley, in southern Nevada and California, United States (fig. 5). A subset of the Mojave Desert, the Amargosa Desert is a hyperarid Basin and Range basin that drains to Death Valley. Mountains up to 2,000 m high surround the Amargosa Desert. At the latitude of the chamber site, the braided channel of the ephemeral Amargosa River and its tributaries occupy nearly the entire 10-kilometer (km) width of the Amargosa Desert floor. The gravelly desert pavement clearly visible in the foreground in figure 2 covers the

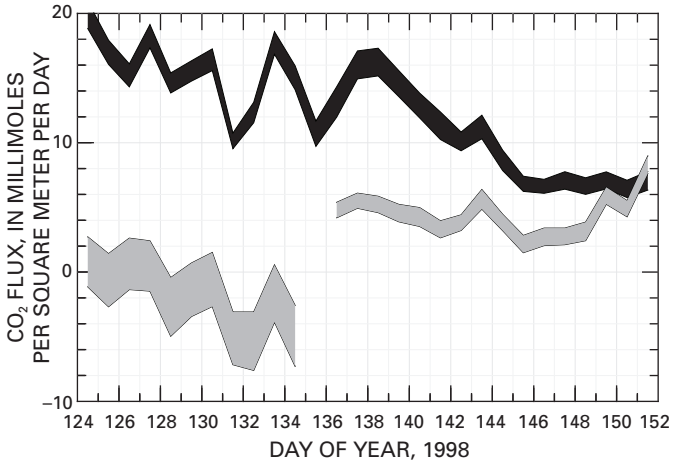

Figure 4. Flux-measurement uncertainties scale with chamber height. Plot breadths are scaled to encompass the 2-σ uncertainty envelopes surrounding opaque-chamber (black band) and clear-chamber (grey band) mean daily fluxes during a short interval in spring 1998. The clear chamber had a tall lid until early DOY 135–136, when a short lid was installed. The opaque chamber had a short lid during the whole interval.

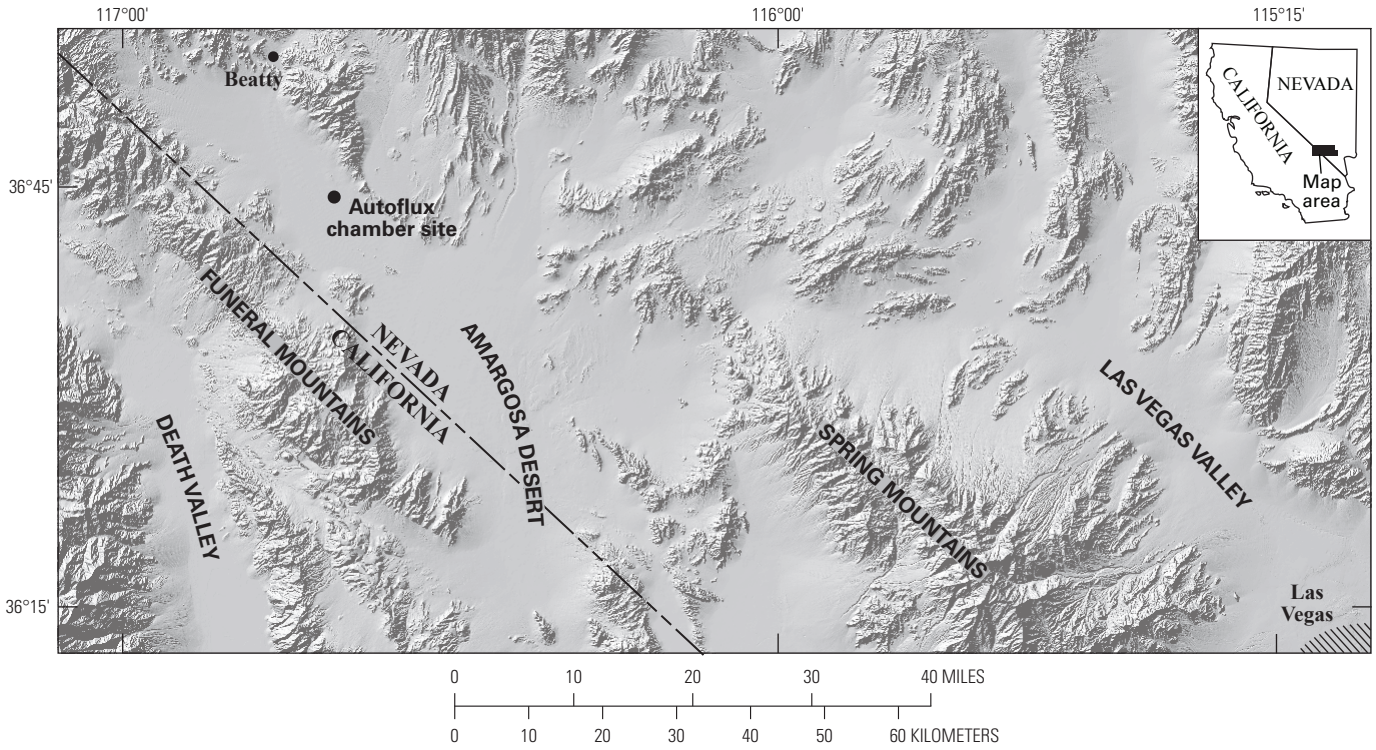

Figure 5. The chamber site (36°44′25″ N, 116°40′57″ W, elevation 820 m) in relation to local and regional topography and State boundaries.

tops of the interfluves between the braids of the ephemeral Amargosa River and its tributaries, all the way to the base of the Funeral Mountains in the distance (fig. 5). The chambers were installed about 3 km southwest of the base of the nearest bajada, at an elevation of about 820 m on the level surface of a kilometer-sized interfluve between the braids of normally dry tributary channels. The soil column at the site is capped by a desert pavement composed of a monolayer of roughly centimeter-sized particles of various lithologies underlain by a 5-cm-thick vesicular horizon of fine-to-medium sand. Below the vesicular horizon, non-vesicular fine-to-medium sand with uncommon coarse sand and pebbles continues to a depth of about 30 cm. A transition from sand to river gravels occurs between 30 and 60 cm, with clean gravels below 60 cm. With the exception of a layer of carbonate-rich coarse sand about 10 cm below the surface, minimal pedogenic carbonate is present (there is about 1 percent calcite in the top 10 cm of the soil), indicating that the near-surface (apparently aeolian) sand layer accumulated in the last 100,000 years (D. Schmidt, U.S. Geological Survey, personal commun., 2000). According to Nichols (1987) and State drilling logs (State of Nevada, 1989, 1994), the substrate from 60 cm to below the approximately 100-m-deep water table is likely to be fluvial boulders and gravel, with lesser amounts of sand, even less silt, and occasional clays. The various size fractions are poorly sorted in some layers and well-sorted in others. Interbedded clay layers at several depths apparently mark lacustrine periods. There is a CO_2-concentration gradient from the water table to the ground surface that, according to a model by D.C. Thorstenson and D.E. Prudic (U.S. Geological Survey, unpub. data, 2002), transports a continuous CO_{2gw} up-flux of about 0.3 mmol m^{-2} d^{-1} across the soil surface. Subsequent, more intensive modeling by Walvoord et al. (2005) arrived at the same flux.

Because the site is located at a relatively low altitude in the Mojave Desert, the climate is notably arid. At a site within 3 km of the CO_2 flux site, the 20-year (yr) (1981–2000) mean annual rainfall was 10.8 cm. Rainfall in 1998 and 1999 was 19.4 cm and 6.8 cm, or approximately 180 percent and 63 percent of the 20-yr mean, respectively (Johnson and others, 2002). At the CO_2 flux site, 16.5 cm of rain fell during 1998, and 5.6 cm fell during 1999. Air temperatures measured during the study ranged between –4° and 46°C.

In the vicinity of the chambers, the normal vegetation was an open stand of perennial creosote bush (*Larrea tridentata*) and little else. During the wet El Niño spring of 1998, many small herbaceous plants of several genera, including multiple species of *Eriogonum* and *Chorizanthe*, sprouted in and around the chambers prior to the April site visit (DOY 97–99). By the May site visit (DOY 135–138), herbaceous plant growth was well-developed (fig. 2) and had probably peaked, as some of the plants in and around the chambers were beginning to yellow. No herbaceous plants grew in or near the chambers at any other time during 1998–1999. During more normal springs, few herbaceous plants grow.

Data Processing and CO_2 Flux Calculation

The first step in data processing was to detect bad flux records and delete them or replace them with interpolated values. Most of the bad records fell into one of four categories: (1) records collected when the pump had failed; (2) periods of battery failure; (3) records where pump-on IRGA instabilities persisted past lid-down; and (4) records having excessively small signal-to-noise ratios, large step changes in CO_2 concentration, or other CO_2 concentration time progressions that are unlikely to have been the result of real CO_2-concentration changes in the chambers.

Pump and battery failures (categories 1 and 2) caused long periods of record loss (DOY 1–12, 1998, and DOY 303–318, 1999) that appear as gaps in the flux chronology. Pump-on IRGA instabilities (category 3) corrupted one to several records in a series. Three or fewer corrupted records in a row were replaced by values interpolated between preceding and succeeding good records. Four or more corrupted records in sequence appear as gaps in the flux chronology. Category 4 bad records tended to occur singly and were replaced with values interpolated between preceding and succeeding good flux records.

As a final quality check on each flux calculation, if the standard error of the CO_2 concentrations around the least-squares best-fit line through the set of points used to evaluate the rate of change of CO_2 in the chambers (described below) exceeded 3.0 ppm, the record was deleted. Fewer than 0.3 percent of the records failed this test. The deleted records tended to occur singly and were replaced with values interpolated from preceding and succeeding good records.

A quirk of the autochamber data was that CO_{2air} concentrations at the beginning of each flux measurement (minute 6, fig. 3) showed consistent diurnal variation that was typically about 20 ppm, but ranged from 10 to 80 ppm. The time course of the CO_{2air} variation superficially resembled the pattern of the CO_2 fluxes, but lagged it, generally by a couple of hours. Correlation coefficients between hourly CO_{2air} concentration and CO_2 flux and *PAR* ranged from 0.33 to 0.38. Correlations between hourly CO_{2air} concentration and all other physical variables were smaller. It is unknown why the measured CO_{2air} concentration varied in such a regular way. In addition, CO_{2air} concentrations tended to be in the 400–500 ppm range at the beginning of each run: the increment above atmospheric concentration (nominally 365 ppm) was probably due primarily to the greater-than-atmospheric pressure needed to move the gas quickly through the sample gas loop. To compensate for the variation in the measured CO_{2air} concentration, all CO_2 concentrations in all runs were normalized to a starting CO_{2air} concentration of 365 ppm.

In numerous runs, the ending CO_{2air} concentration (minute 12, fig. 3) differed from the starting free-air concentration (minute 6, fig. 3), apparently because of instrumental drift. To compensate for drift, readings made after lid drop were adjusted by an amount proportional to the time after lid-drop, so that the average of the last three free-air readings was 365 ppm, the same as the normalized CO_{2air} concentration at the beginning of the run. Soil CO_2 flux was then calculated as follows:

$$CO_2\ flux = slope \times height \times \frac{barpress}{1013.25} \times \frac{273.15}{temp + 273.15} \times 64.25 \qquad (1)$$

where

$CO_2\ flux$ is in millimoles per square meter per day;

slope is the rate of change of CO_2 concentration in the chamber in parts per million per minute (ppm min^{-1});

height is effective chamber height in meters;

barpress is barometric pressure in millibars;

temp is air temperature in degrees Celsius (°C);

and

the constant (64.25) converts ppmv min^{-1} to mmol m^{-2} d^{-1}.

Because thousands of fluxes were measured in this study, we developed an automated method of calculating flux from the measured CO_2 concentrations. The goal was to extract the maximum slope of the CO_2 concentration curve. Initially, the least-squares best-fit line through all possible same-sized groups of contiguous CO_2 measurements was calculated from group sizes ranging from three to eight. Then the slope of the best-fit line with the maximum absolute value was chosen to calculate the flux for that record. This approach was abandoned because (1) downward fluxes (discussed in the "Fluxes from Hot Dry Soil" section) could not be calculated; (2) it selected for groups which had aberrant CO_2 measurements at their ends, which yielded artificially large slopes; and (3) no near-zero fluxes were calculated. For these reasons, the fluxes in Riggs and others (1999), which were calculated using this approach, should not be used.

The fluxes presented here were calculated using the slope of the best-fit line through 21 consecutive CO_2 measurements, beginning with the fourth measurement after lid down (the first CO_2 measurement that was distinctly above atmospheric concentration after lid down on high-flux days) and ending with the first measurement after lid up (the last measurement before CO_2 concentration began to fall after lid up on high-flux days). This computational approach yields a more stable and well-behaved flux time series than results when fewer CO_2 measurements are used to calculate the fluxes. An undesirable consequence of this computational approach is that it presumably underestimates the real fluxes by the amount the average slope of CO_2 concentration change during the 3.5-min measurement interval diverges from the instantaneous slope at lid down. While underestimation of fluxes is undesirable, it has a minor effect on the temporal variation of flux and renders conclusions based on flux variations that are more conservative than they would otherwise be. Rochette and Hutchinson (2005) present this as a viable computational approach that is not as sensitive to measurement imprecision as nonlinear flux models.

The uncertainty inherent in individual flux measurements tends to obscure the actual temporal variations of flux, the partitioning of total flux between CO_2 different sources, and the relationships between flux and other environmental variables. The uncertainties were substantially reduced by constructing ensemble fluxes, that is, averages of tens of individual flux measurements made under substantially similar conditions. The ensembles of fluxes and other physical variables presented in this report are averages of measurements made at the same time of day on cloudless days when soil moisture and temperature were within predetermined ranges. Correlation coefficients of ensemble data were calculated from the values of different variables compared at the same time of day.

Laboratory CO_2 Adsorption Experiments

Some of the measured flux progressions appeared to be caused by temperature-controlled adsorption/desorption of CO_2 onto/off of soil grains. To test the feasibility of such a mechanism, evaluation of the temperature dependence of CO_2 adsorption onto Amargosa Desert soil was performed in a surface-area analyzer (D. Rutherford, U.S. Geological Survey, unpub. data, 2005). The soil sample was collected as a core of the top 8 cm of the soil column. The sample, 588 g of soil with a bulk density of 1.40 grams per cubic centimeter, was sieved through a 2-mm screen, and the >2-mm particles (56 g) were discarded. Three 10-g subsamples of the <2-mm fraction of bulk soil were prepared by heating at 100°C in a 10 milliliters per minute (mL min^{-1}) stream of ultra-high-purity helium gas for a minimum of 16 hrs before each analysis. Carbon dioxide uptake by the soil samples was measured relative to uptake by an empty reference tube at 10 pressures of CO_2 ranging from $10^{-1.93}$ to $10^{-0.93}$ atmospheres (atm). Correction was made for the free space difference between the sample tube and the reference tube. Uptake was converted to milliliters per gram at standard temperature and pressure. Adsorption isotherms were measured at 0°, 10°, 20°, and 30°C; CO_2 uptake was 1.05, 0.54, 0.29, and 0.27 micromoles per gram of soil. The adsorption isotherm at each temperature was fitted to a Freundlich isotherm (Freundlich, 1926), which was used to extrapolate the CO_2 uptake to the atmospheric partial pressure of CO_2 (P_{CO_2}), or $10^{-3.44}$ atm at the time the analyses were done (fig. 6).

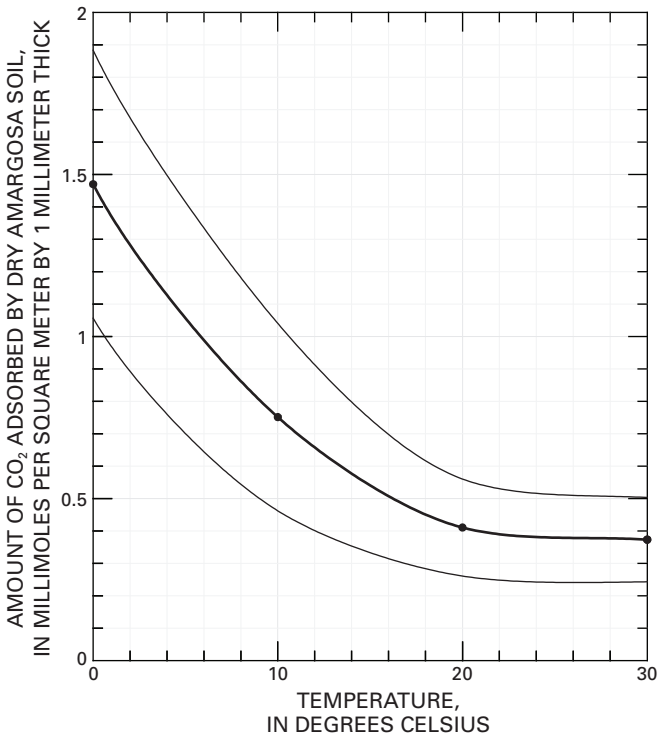

Figure 6. CO_2 adsorption onto the <2-mm-diameter fraction of dry Amargosa Desert soil in a pure CO_2 atmosphere at $10^{-3.44}$ atm, as a function of temperature. The fine black lines mark the 1-σ uncertainties around the mean values of three runs.

Soil CO_2 Flux

Fortuitously, the 2 yrs of flux and ancillary measurements were made during abnormally wet El Niño 1998 and unusually dry La Niña 1999, so the results reported here span most of the range of weather conditions, especially precipitation, that make up the Amargosa Desert's present climate. Annual, daily, and hourly fluxes will be presented and discussed in terms of sizes, mechanisms, and CO_2 sources.

Annual Fluxes

Mean annual opaque-chamber flux was more than an order of magnitude larger in El Niño 1998 than in La Niña 1999 (table 1), indicating that total soil CO_2 production was strongly enhanced by the abnormally abundant El Niño precipitation. However, mean annual clear-chamber flux was only slightly larger in El Niño 1998 than in La Niña 1999, indicating that a large portion of the excess El Niño flux was recaptured and photosynthetically converted back into organic compounds. Had a sample of the above-ground parts of perennial plants growing in the vicinity of the chambers been included inside the chambers in proportion to their areal coverage, the El Niño opaque-chamber flux probably would have been larger and the clear-chamber flux smaller, or even downward, given that wet years are likely to be the primary times when the small pool of organic carbon in the Amargosa Desert soil is replenished.

When measurement and modeling uncertainties are taken into account, the La Niña 1999 opaque-chamber flux of 0.4 mmol m^{-2} d^{-1} is indistinguishable from the 0.3 mmol m^{-2} d^{-1} CO_{2gw} flux, suggesting that little CO_{2biol} was produced in 1999. The La Niña opaque-chamber flux is only a fifth of the clear-chamber flux (table 1), an offset opposite the direction attributable to photosynthesis and explicable only as a soil-heating effect, which will be discussed in the "Hourly Fluxes" section.

Table 1. Mean annual CO_2 fluxes, rainfall, and soil temperature during El Niño 1998 and La Niña 1999.

[mmol m^{-2} d^{-1}, millimoles per square meter per day; cm, centimeter; °C , degrees Celsius]

	El Niño 1998	La Niña 1999
Opaque-chamber flux (mmol m^{-2} d^{-1})	4.7	0.4
Clear-chamber flux (mmol m^{-2} d^{-1})	3.4	2.0
Total annual rainfall (cm)	16.45	5.60
Mean annual soil temperature (°C at 5-cm depth)	22.5	23.1

Mean annual fluxes measured during this study (table 1) were small compared to:

- The 8.2 mmol m^{-2} d^{-1} flux that McConnaughey (cited in Walvoord and others, 2005) measured at a site about 3 km from, <30 m higher than, and geologically and botanically very similar to the autochamber site. Because no information is presented on the equipment or measurement protocol used, there is little basis on which to compare the measurements.

- The 9.6 mmol m^{-2} d^{-1} flux that Thorstenson and others (1998) calculated from the subsurface CO_2 profile adjacent to the Jackass Flats caisson, about 30 km from and 330 m higher than the autochamber site. The Thorstenson and others (1998) flux is about twice as large as the El Niño opaque-chamber annual flux and about 20 times as large as the La Niña opaque-chamber annual flux (table 1). The difference between the Jackass Flats and autochamber fluxes probably results from a combination of (1) real differences between the fluxes due to the effective moisture and soil differences between the two sites; (2) uncertainties in the tortuosity used to calculate the Jackass Flats flux, which is thought to be accurate to a factor of two or three (E. Weeks, U.S. Geological Survey, personal commun., 2006); and (3) the conservative approach used to calculate the autochamber fluxes.

- The 51±8.7 mmol m^{-2} d^{-1} flux Raich and Schlesinger (1992) present as characteristic of fluxes from desert scrub, the hottest xeric environment listed in their compilation of soil CO_2 fluxes typical of the range of global terrestrial climates. The Raich and Schlesinger (1992) number is much larger than either of the long-term fluxes measured in the Amargosa Desert, primarily because it is based on measurements from less arid sites. This difference is important because an overestimate of fluxes from hot deserts (which occupy about a fifth of the earth's land area) predisposes overestimation of the arid component of total global flux.

In summary, fluxes from the Amargosa Desert are small, no matter what measurement methodology is used, and for reasons that cannot be determined from the annual flux data, wet years produce larger opaque-chamber fluxes and dry years produce larger clear-chamber fluxes.

Daily Fluxes

1999 La Niña Fluxes

With four exceptions, mean daily fluxes were small (≤5 mmol m^{-2} d^{-1}) throughout dry La Niña 1999 (fig. 7). Slightly larger fluxes in spring and early summer (DOY 90–180), relative to winter (DOY 1–60, 330–365), probably resulted from the soil warming to a depth where soil moisture was sufficient to support a minor increase in soil CO_{2biol} production; however, this is conjectural because the soil moisture profile was not measured. Larger clear- than opaque-chamber fluxes, as noted in the "Annual Fluxes" section above, were most pronounced in the summer when the soil was hot and dry (fig. 7). The four exceptions, large flux spikes that peaked on DOY 191, 196, 222, and 260 and stayed elevated a total of 10 days, were responses to rainfall on hot dry soil. The small flux response to a rain that increased cool-soil moisture by 11 percent on DOY 24 shows that rainfall alone was insufficient to elicit large fluxes. The daily flux data provide no insight into the mechanism(s) responsible for the offset or the different hot-soil and cool-soil responses to rainfall.

1998 El Niño Fluxes

Opaque Chamber, First Half of 1998

In early February 1998, the first of a series of rains increased soil moisture to 22 percent, and succeeding rains kept soil moisture continuously above 12 percent through mid-May. During this time, CO_2 flux tracked soil temperature's upward zigzag, topping out at 20 mmol m^{-2} d^{-1} in early May (DOY 125), when mean daily soil temperature at 5-cm depth was 24°C (fig. 8). The correlation coefficient (r) between CO_2 flux and mean soil temperature was 0.95 from February through mid-May (DOY 32–136), while the r between CO_2 flux and soil moisture during the same period was –0.77, suggesting that, so long as soil moisture was greater than or equal to (≥) 12 percent, flux was primarily a function of temperature. The flux Q_{10} (Q_{10} is the factor by which flux changes in response to a 10°C rise in temperature) from February through mid-May was approximately 4.25, although the data points do not form a purely exponential distribution (fig. 9). Davidson and others (1998) point out that the real-world relation between flux and temperature tends not to be purely exponential because, for example, the ratio of microbial to root respiration can change with temperature, fluxes from different soil horizons can have different temperature responses, and soil moisture content (which often covaries with temperature) also can affect fluxes.

Mean daily soil temperature continued to rise until DOY 200 (19 July), reaching 45°C, but opaque-chamber fluxes began a steep decline around DOY 138 as soil moisture dropped rapidly below 12 percent. From DOY 136 to 200, opaque-chamber fluxes followed the trend of decreasing soil moisture (r = 0.74) and were negatively correlated with changes in temperature (r = –0.66). Thus, the relation between

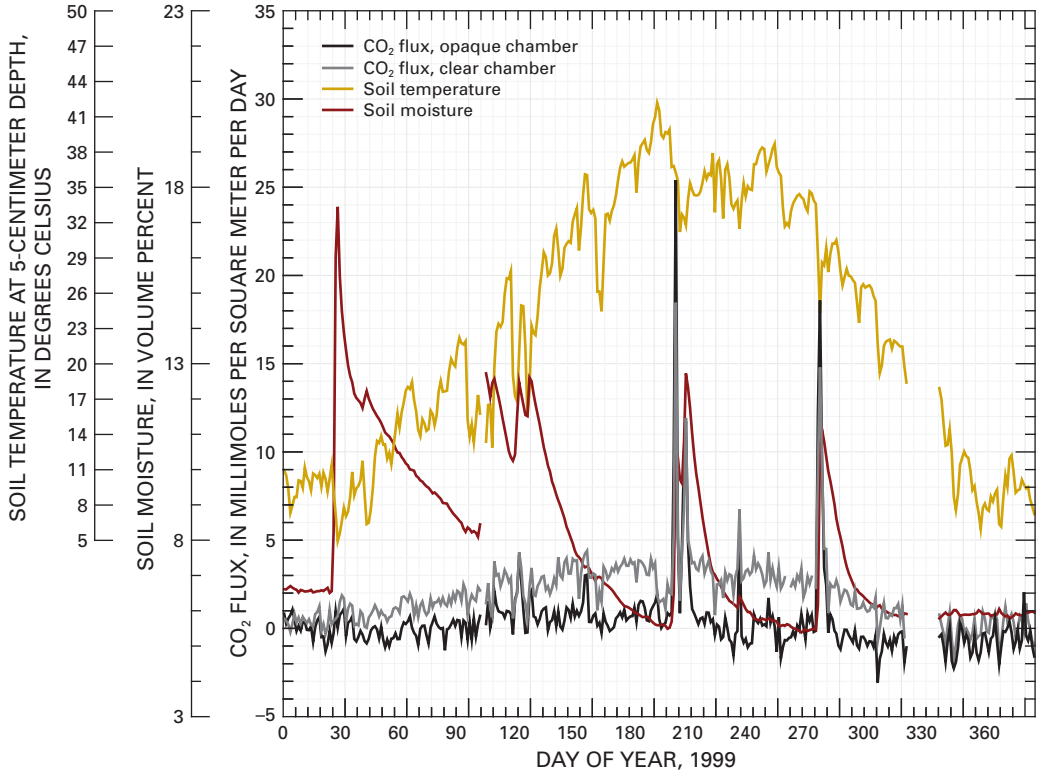

Figure 7. Mean daily clear- and opaque-chamber CO_2 fluxes, soil temperature, and soil moisture during dry La Niña 1999.

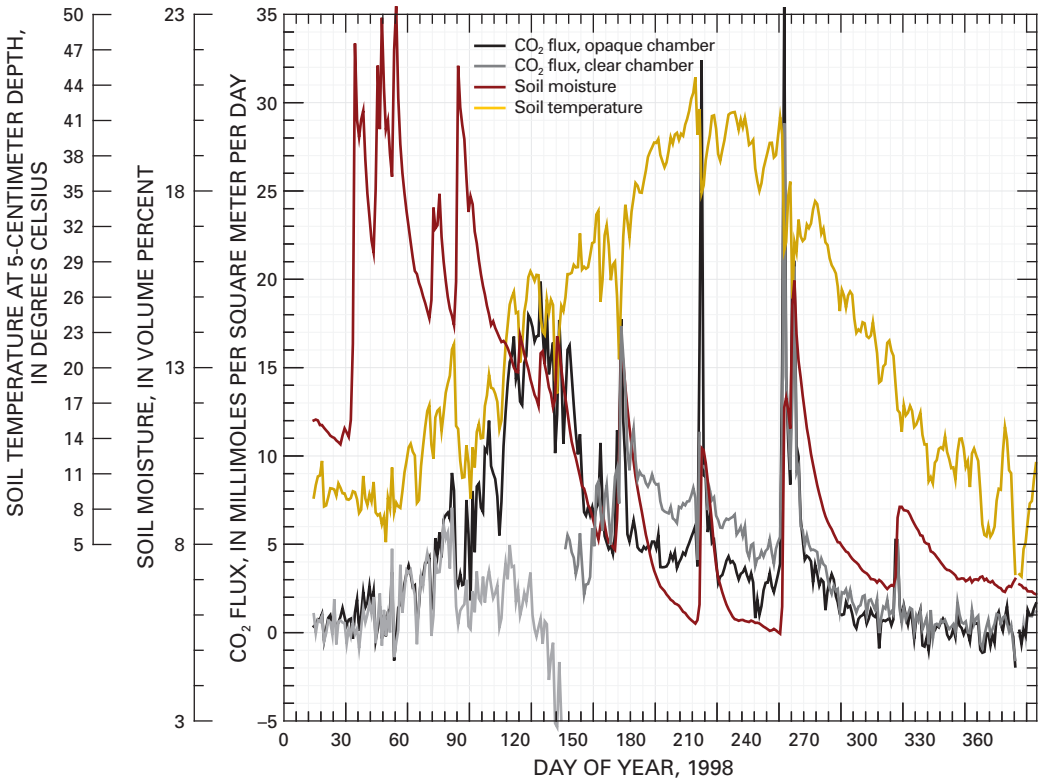

Figure 8. Mean daily clear- and opaque-chamber CO_2 fluxes, soil temperature, and soil moisture during wet El Niño 1998. The large clear-chamber flux discontinuity at DOY 136 marks the switch from a tall chamber lid to a short one.

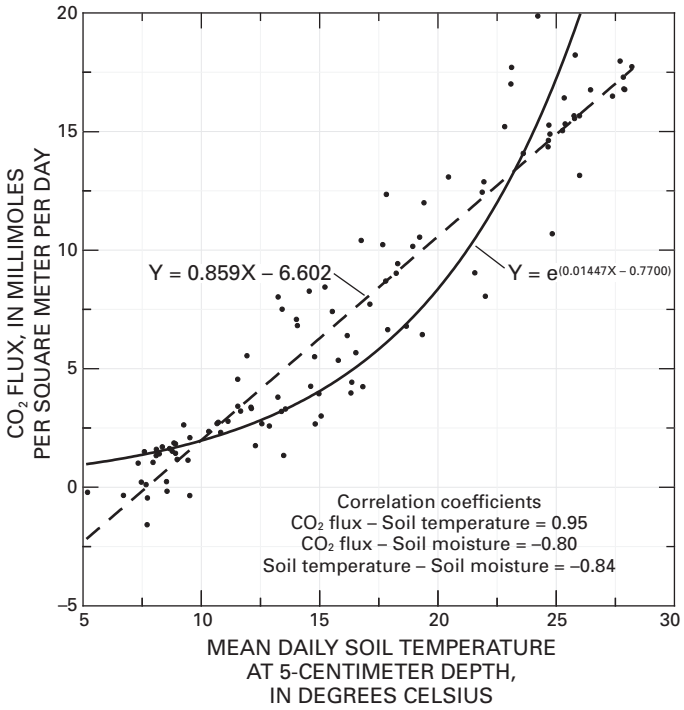

Figure 9. Mean daily fluxes at a time when soil moisture was not limiting (February through mid-May 1998) plotted against mean daily soil temperature at a depth of 5 centimeters. Linear and exponential best-fit lines and equations also plotted.

flux and soil moisture was a threshold response. When soil moisture was greater than the 12 percent threshold concentration, CO_{2biol} production in the soil was not water-limited, and the amount of CO_{2biol} produced was a positive function of temperature. Below the moisture threshold, CO_{2biol} production in hot soil was limited by, and a positive function of, soil moisture content. Davidson and others (1998) note that flux in the Harvard Forest (Petersham, Mass., United States) also exhibits threshold behavior with regard to soil moisture, in that below the 12 percent threshold CO_2 flux decreases rapidly with decreasing soil moisture.

Clear Chamber, First Half of 1998

From mid-January (DOY 14) through late March (about DOY 90), clear-chamber fluxes were comparable to opaque-chamber fluxes (fig. 8). In late March, as opaque-chamber fluxes began to rise sharply, clear-chamber fluxes remained relatively constant, oscillating in the 0–5 mmol m^{-2} d^{-1} range until early- to mid-May, when clear-chamber fluxes fell to –5.0 mmol m^{-2} d^{-1} (fig. 8). The divergence between clear- and opaque-chamber fluxes marks the onset of photosynthetic uptake of CO_{2air} in the clear chamber by tens of small herbaceous plants, mostly species of *Chorizanthe* and *Eriogonum*, that had sprouted and were growing in both chambers at the time of site visits in early April (DOY 98) and mid-May (DOY 136) (fig. 10). The magnitude of the divergence between clear- and opaque-chamber fluxes (that is, the amount of photosynthetic uptake of CO_{2air}) increased until about DOY 126. From DOY 126 to 135, the divergence was at its maximum, ranging from 15 to 20 mmol CO_2 m^{-2} d^{-1}. From DOY 137 to 151, the divergence rapidly shrank to 0, signaling the death of the plants and the end of photosynthetic uptake of CO_{2air} in the chambers. The jump in clear-chamber flux when the tall lid was replaced with a short lid (fig. 8, DOY 135–137) suggests that there was a calibration difference between the two lid heights, but the similarity of tall clear- and short opaque-chamber fluxes at the beginning of 1998 argues against large calibration differences. Hence, it appears that the flux jump was primarily caused by desiccation of the plants in the chamber in response to the rapid decrease of soil moisture through the 12 percent threshold concentration at the time of the lid swap.

A

B

Figure 10. Numerous small plants, mostly species of *Chorizanthe* and *Eriogonum*, grew in the chambers for about 2 months during spring 1998. *A*, Opaque chamber plants, April 8 (DOY 98) 1998. The greens have been digitally intensified to make the plants more visible. *B*, Opaque chamber plants, May 16 (DOY 136) 1998. Because the greens have been digitally intensified to make the plants more visible, it is not apparent that many of the plants inside and outside the chamber were beginning to yellow.

Both Chambers, Last Half of 1998

As the soil progressively dried during the last half of 1998, CO_2 flux converged on the 1999 pattern (figs. 7, 8) in three different ways: (1) summer and fall rains stimulated abrupt short-term releases of large amounts of CO_2; (2) clear-chamber flux substantially exceeded opaque-chamber flux, so long as soil moisture was <10 percent; and (3) during the last 48 days of both years, clear- and opaque-chamber fluxes were small and varied similarly.

Hourly Fluxes

Hourly measurements of flux and the other environmental variables provide a record of sufficient temporal resolution that the different CO_2 sources and biophysicochemical mechanisms contributing to the fluxes can be inferred. In this section, such inferences will be attempted for the four sets of soil temperature and moisture extremes—warm moist, cool moist, hot dry, and cool dry. Fluxes under most other sets of conditions, as well as the mechanisms controlling them, are intergrades between the extremes.

Fluxes from Warm Moist Soil

This discussion of fluxes from warm moist soil is based on an ensemble (fig. 11*A*) of 20 cloudless days in the spring of 1998. Ensemble mean soil temperature at 5-cm depth was 23.4°C, with the mean temperatures of the individual ensemble days ranging from 14.1° to 28.2°C. Ensemble mean volumetric soil moisture in the top 10 cm of the soil was 13.4 percent, with mean soil moisture of the individual days ranging from 12.1 to 15.1 percent; therefore, soil moisture was always greater than the 12 percent threshold concentration.

The opaque chamber flux, which was the largest sustained flux measured (table 2), was continuously upward, with a steep morning rise, a broad rounded midday peak, a steep afternoon decrease, and a slow nocturnal decrease. Compared to opaque-chamber flux, clear-chamber flux was smaller and more irregularly variable (fig. 11*A*). The smaller clear-chamber daytime fluxes are due to photosynthetic CO_2 uptake by the tens of small plants that grew in the chambers throughout the ensemble interval. The irregular variability and smaller nocturnal fluxes apparently stem from calibration differences between the clear chamber's tall lid and the opaque chamber's short lid during the ensemble. When both chambers had short lids, as during the hot dry or cool dry ensembles described in the "Fluxes from Hot Dry Soil" section and the "Fluxes from Cool Dry Soil" section, both chambers' nocturnal fluxes were very similar, and clear- and opaque-chamber ensembles varied equally smoothly. This suggests that clear- and opaque-chamber nocturnal fluxes from warm moist soil were actually about the same, and that raising the clear-chamber ensemble curve so that its nocturnal fluxes equal opaque-chamber nocturnal fluxes may provide a better estimate of clear-chamber ensemble flux.

The large opaque-chamber ensemble flux is consistent with the conventional wisdom (for example, Raich and Schlesinger, 1992) that fluxes tend to be largest when soil conditions are simultaneously warm and moist, that is, most favorable to biological activity. Clear-chamber ensemble flux is basically opaque-chamber flux minus the photosynthetic uptake of CO_{2air}. Hence, metabolic CO_{2biol} production in the soil and photosynthetic uptake of CO_{2air} may be entirely responsible for the amount and timing of CO_2 fluxes from warm moist soil. Before accepting this proposition, however, the potential for flux contributions by non-biological mechanisms will be evaluated.

Four non-biological mechanisms can potentially contribute to fluxes at the chamber site: down-flux of CO_{2air} into the soil; up-flux of CO_{2gw} exsolved from the water table; release of CO_2 as near-surface soil water evaporated; and CO_2 exsolution from/dissolution into near-surface soil water in response to temperature changes. Because CO_2 flux was almost continuously upward, there was no significant down-flux of CO_{2air} into warm moist soil. The 0.3 mmol m^{-2} d^{-1} up-flux of CO_{2gw} from the water table was a constant component of flux, but at only about 2 percent of total opaque-chamber flux, it was an insignificant contributor to total flux. The following sections discuss CO_2 exsolution from evaporating soil water and temperature-mediated CO_2 exsolution from/dissolution into soil water.

CO_2 Release by Evaporating Soil Water

Integration of the area under the *ET* curve in figure 11*A* indicates that about 2.4 liters per square meter per day (L m^{-2} d^{-1}) of soil water were lost to *ET*. It is unknown how *ET* was partitioned into *E* and *T*, but about 3 km from the flux chamber site, *E* was found to be 60 percent of *ET* on a cloudless day (M.J. Johnson and B.J. Andraski, U.S. Geological Survey, unpub. data, 2005) when *ET* was 25 percent of that on the ensemble day. Using Johnson and Andraski's partitioning, *E* at the chamber site would have been about 1.4 L m^{-2} d^{-1}. According to the geochemical modeling program PHREEQC (Parkhurst and Appelo, 1999), at a temperature of 12°C (the lowest soil temperature shown in fig. 11*A*), an estimated soil gas P_{CO_2} of $10^{-3.0}$ atm, and equilibrium with solid calcite, the 1.4 L of soil water could dissolve (and hence release on evaporation) about 1.3 mmol of CO_2. Thus, CO_2 released as soil water evaporated could have contributed up to 9 percent and 52 percent of the total daily clear- and opaque-chamber up-fluxes, respectively (table 2). The time course of CO_2 release by evaporating soil water was probably similar to that of the *ET* curve (fig. 11*A*). If so, the approximately 0.16 L m^{-2} hr^{-1} of water potentially lost to *E* at peak midday *ET* released CO_2 at a maximum rate of 3.6 mmol m^{-2} d^{-1}, or 13 percent and 45 percent of clear- and opaque-chamber maximum midday up-fluxes, respectively. Like *ET*, evaporative CO_2 contributions to flux would have ramped up before noon, down after noon, and been negligible at night (fig. 11*B*).

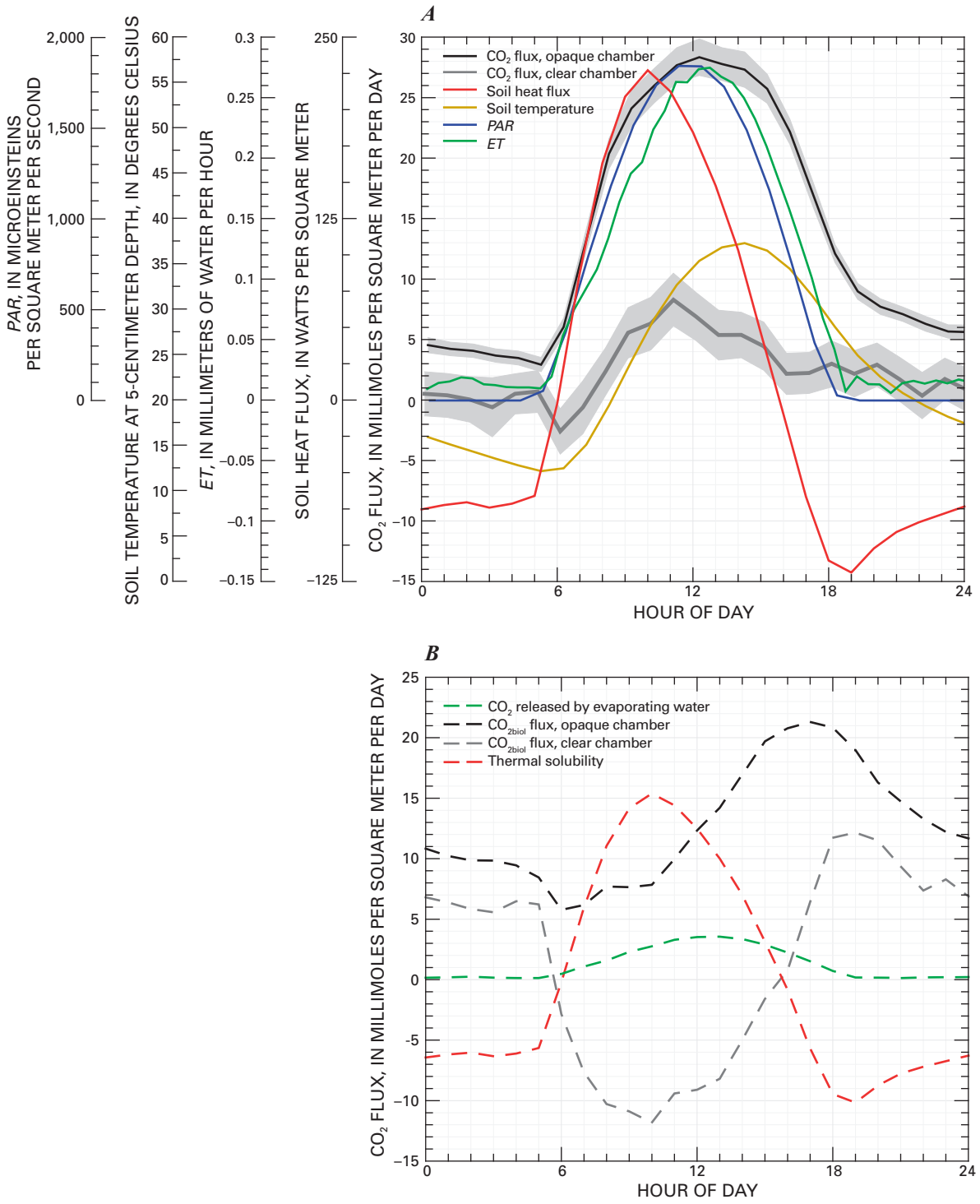

Figure 11. Ensemble CO_2 fluxes and other physical variables from warm moist soil. *A*, Clear- and opaque-chamber fluxes (the light gray band surrounding the CO_2-flux curves is the 2-σ uncertainty envelope), soil temperature, soil heat flux, photosynthetically active radiation (*PAR*), and evapotranspiration (*ET*). *B*, Estimates of the components of the total flux contributed by instantaneous CO_{2biol} production, CO_2 released/taken up as soil water evaporated/condensed, and CO_2 thermal solubility. The instantaneous CO_{2biol} production curve is the remainder after the CO_2 flux components contributed by evaporating water and thermal solubility, as represented by the curves in figure 11*B*, are subtracted from the total CO_2 flux curves in figure 11*A*.

Table 2. Size and timing of various physical variables related to CO_2 fluxes under soil moisture and temperature extremes.

[Ensemble fluxes are calculated as the average hourly fluxes of multiple cloudless days (20, 53, and 36, for the warm moist, hot dry, and cool dry ensembles, respectively). Non-ensemble fluxes are calculated as bulk average fluxes of 24 variably cloudy days. The fluxes in parentheses were measured when the clear chamber had a tall lid. mmol m^{-2} d^{-1}, millimoles per square meter per day; %, percent; °C, degrees Celsius; mL, milliliters; temp, temperature; Vasc, vascular plants; BSC, biological soil crust; --, indicates values that would be misleading to calculate under non-ensemble conditions; Opq, opaque chamber; Clr, clear chamber]

Type of measurement	Ensemble						Non-ensemble	
Soil conditions	Warm Moist		Hot Dry		Cool Dry		Cool Moist	
Chamber type	Opq	Clr	Opq	Clr	Opq	Clr	Opq	Clr
Total daily flux (mmol m^{-2} d^{-1})	14.0	(2.5)	2.0	4.5	0.1	0.4	1.1	(0.8)
Daytime upflux (mmol m^{-2} d^{-1})	14.0	(2.5)	2.8	5.6	1.4	2.1	1.2	(1.5)
CO_{2air} downflux (mmol m^{-2} d^{-1}/% of daytime upflux)	0.0/0	(0.0/0)	–0.8/29	–1.1/20	–1.3/93	–1.7/81	–0.3/25	(–0.9/60)
CO_{2gw} (mmol m^{-2} d^{-1}/% of daytime upflux)	0.3/2	0.3/(14)	0.3/11	0.3/5	0.3/21	0.3/14	0.3/25	0.3/(20)
CO_{2biol} (mmol m^{-2} d^{-1}/% of daytime upflux)	13.7/98	(2.1/86)	1.7/61	4.2/75	–0.2/–14	0.1/5	0.6/50	(0.3/20)
Mean soil moisture (volume %)	13.4		6.0		6.8		19.5	
Soil temperature (mean temp at 5 cm, °C)	23.4		38.0		9.3		8.5	
Daily maximum temperature at 5 cm depth (time of day)	14:15		14:10		14:15		--	
Daily minimum temperature at 5 cm depth (time of day)	5:40		5:45		7:20		--	
Total daily *ET* (mL m^{-2} d^{-1})	2,380		536		105		--	
Daily upward *ET* (mL m^{-2} d^{-1})	2,380		595		225		--	
Daily downward *ET* (mL m^{-2} d^{-1})	0		–63		–120		--	
Photosynthesis	No	Vasc	No		No		No	BSC?
Chamber artifact (daily fluxes)	Nocturnal tall chamber		Clr = 2.2 × Opq		Clr = 5.25 × Opq		Nocturnal tall chamber	
Cloudiness	None		None		None		Partly cloudy	

Temperature-Controlled Soil-Water CO_2 Dissolution/Exsolution

The solubility of gases in liquids is an inverse function of temperature, so CO_2 tends to exsolve from soil water as the soil warms during the day and dissolve into soil water as the soil cools during the night. The potential contribution of this mechanism to the ensemble flux can be estimated from the 12°–36°C daily soil temperature range (fig. 11*A*). Assuming a soil moisture content of 12.0 L m^{-2} in the top 10 cm (13.4 percent volumetric soil moisture, or 13.4 L m^{-2}, minus the 1.4 L m^{-2} d^{-1} that evaporated), a soil gas P_{CO_2} of 10^{-3} atm, and equilibrium with solid calcite, PHREEQC indicates that 11.3 and 7.4 mmol m^{-2} of CO_2 would dissolve at 12°C and 36°C, respectively. The difference, 3.9 mmol m^{-2}, is an estimate of the amount of CO_2 that exsolved/dissolved daily in response to temperature cycling. To the extent that CO_2 exsolution/dissolution was in proportion to the magnitude of soil heat flux (that is, the rate at which the soil was heating/cooling), the estimated size and timing of CO_2 contributions to hourly flux could have been as shown in figure 11*B*. Temperature-controlled CO_2 exsolution/dissolution would have had the primary effect of bolstering flux between the hours of 6:00 and 15:45 and diminishing flux the rest of the time (fig. 11*B*), but because there was little net change in soil temperature from the beginning to the end of the ensemble day (fig. 11*A*), soil water acted as a reversible thermally mediated CO_2 reservoir that contributed minimally to total daily flux.

Biologically Mediated Flux Component

If the amounts of CO_2 estimated to have exsolved/dissolved in response to temperature change and soil-water evaporation are subtracted from the ensemble fluxes, the remainder is an estimate of the production rate of the biologically mediated component of the flux, that is CO_{2biol} production in the soil and photosynthetic CO_{2air} uptake combined (fig. 11*B*). Because darkness inhibits photosynthesis, the opaque chamber's biologically mediated flux should be composed entirely of CO_{2biol}, and the shape of the curve should approximate the time course of CO_{2biol} production in the soil (fig. 11*B*). Peak opaque-chamber CO_{2biol} production lagged peak soil temperature at 5-cm depth by nearly 3 hrs and was more constant than the opaque-chamber ensemble flux, suggesting that greatest CO_{2biol} production occurred at least several centimeters below the soil surface (fig. 11*B*).

The clear-chamber biologically mediated CO_2 flux curve (fig. 11*B*) is the summation of metabolic CO_{2biol} production and photosynthetic CO_{2air} uptakes. Whether the clear-chamber curve is raised until its nocturnal fluxes equal those of the opaque chamber or not, the daytime clear-chamber biological flux component is downward, indicating that during the day, photosynthetic CO_{2air} uptake by the tens of herbaceous vascular plants that grew in both chambers throughout the ensemble (fig. 10) exceeded metabolic CO_{2biol} production, as would be expected during the rare times when soil organic carbon has the potential to be replenished. The net daytime down-flux of biologically mediated carbon is masked in the

ensemble clear-chamber curve, primarily by exsolution of CO_2 as soil water heated during the day, giving the false impression that, even during El Niño conditions, metabolic CO_{2biol} release always exceeded photosynthetic CO_{2air} uptake.

Summary

Warm moist soil was favorable to biological activity, producing by far the largest sustained opaque-chamber flux. The opaque-chamber flux was continuously upward with a broad midday peak, while clear-chamber flux resembled the opaque-chamber flux with the midday peak depressed by photosynthetic CO_2 uptake. The shapes of the flux curves might be interpreted entirely as a consequence of the timing of CO_{2biol} production and photosynthetic CO_{2air} uptake, but CO_2 exsolution as soil water evaporated around midday and reversible temperature-controlled CO_2 exsolution/dissolution likely also made substantial contributions to the shape of the total flux curves. If so, opaque-chamber CO_{2biol} production peaked in the late afternoon and was relatively constant, suggesting that the focus of CO_{2biol} production was at a depth of several centimeters. Assuming similar CO_2 exsolution fluxes, clear-chamber CO_{2biol} flux was downward during midday, indicating that photosynthetic CO_{2air} uptake exceeded CO_{2biol} production in the soil.

Fluxes from Cool Moist Soil

There was an insufficient number of full-sun days when the soil was cool and moist to make a meaningful ensemble of cool-season full-sun fluxes from moist soil. However, from February 4 to 27 (DOY 35–58), 1998, there was a series of typically partly cloudy days when the mean soil moisture was 19.5 percent and the mean soil temperature at 5-cm depth was 8.5°C (fig. 12). This discussion of cool-season moist-soil fluxes is based on observations gleaned from this 24-day period, without regard for the effects of cloudiness, so the characterization of cool-season moist-soil fluxes is not methodologically comparable to the full-sun ensembles used to characterize fluxes from other sets of conditions. The clear chamber was equipped with a tall lid during February 1998, so clear-chamber fluxes exhibit instabilities and artifacts similar to those in the warm moist soil ensemble. Despite that, clear- and opaque-chamber hourly fluxes varied similarly (fig. 12). Important features of cool-moist-soil fluxes are discussed in the next three sections.

Daytime Up-Flux, Small Nocturnal Up- and Down-Fluxes

Cool moist soils tended to exhibit a pattern of daytime up-fluxes peaking about noon and relatively small nocturnal up- and down-fluxes (fig. 12). During daylight hours (the 10.68 hours per day [hr d^{-1}] when *PAR* was ≥10 microEinsteins per square meter per second [μE m^{-2} s^{-1}]), opaque-chamber fluxes had a correlation of 0.69 with both *PAR* and soil temperature at a depth of 5 cm, while clear-chamber fluxes had correlations with *PAR* and soil temperature of 0.58 and 0.54, respectively. Furthermore, short cloudy periods during the day often caused short-term flux decreases, particularly in the opaque chamber (fig. 12). These responses indicate that, similar to warm moist soil, daytime CO_2 up-flux from cool moist soil was stimulated primarily by solar soil warming.

The opaque-chamber's nighttime flux (the 13.32 hr d^{-1} when *PAR* was <10 μE m^{-2} s^{-1}) of –0.2 mmol m^{-2} $night^{-1}$ may be the result of increases in CO_2 solubility as soil water cooled, or, given that the correlation between flux and soil temperature at 5 cm depth was only 0.11, may be mostly a chamber artifact. The –0.5 mmol m^{-2} $night^{-1}$ clear-chamber nocturnal flux is probably mostly a tall-lid artifact.

Down-Fluxes during Rains, Small Fluxes Afterward

For the duration of each of the four largest rains in February 1998, as indicated by sharp increases in soil moisture (fig. 12), opaque-chamber fluxes were, with a few minor exceptions, downward (spiking down to –7.5 mmol m^{-2} d^{-1}), even at midday when peak up-fluxes usually occurred (fig. 12). Clear-chamber hourly fluxes likewise tended to be downward during the rains, but with numerous exceptions that were probably tall-chamber artifacts. The down-fluxes were not caused by rain creating an ephemeral saturated-zone barrier to gas movement at the soil surface, nor were they the result of low P_{CO_2} rainwater intercepting soil CO_2, because both processes could only reduce fluxes, not reverse them. A mechanism that can account for the CO_2 down-fluxes during the rainfalls is the increase in CO_2 solubility that accompanies dissolution of soil calcite into infiltrating rainwater. At atmospheric P_{CO_2} and temperatures of 5° and 20°C, CO_2 solubility increases, according to PHREEQC (Parkhurst and Appelo, 1999), by factors of 28 and 37, respectively, when pure water is equilibrated with solid calcite. The day or more of small erratic near-zero fluxes that typically followed rain on cool moist soil are probably a consequence of the time required for the soil to produce enough CO_2 to saturate the infiltrated rainwater.

Larger Fluxes than Cool Dry Soil

February 1998 opaque-chamber fluxes from cool moist soil exceeded opaque-chamber fluxes from cool dry soil by a factor of 11, even though the cool moist soil was 0.8°C cooler at 5-cm depth than the cool dry soil (table 2). This suggests that CO_{2biol} production was substantially enhanced by the increased soil moisture. The factor of 11 is probably conservative because CO_2 flux from cool moist soil would have been even larger under full-sun conditions. Cool-moist-soil clear-chamber fluxes exceeded cool-dry-soil clear-chamber fluxes by a factor of only 2 (0.8 versus 0.4 mmol m^{-2} d^{-1}). The relatively small difference was probably due to an overestimate of flux typical of the clear chamber on dry soil (discussed in the "Fluxes from Hot Dry Soil" section), possibly augmented by photosynthetic CO_{2air} uptake by biological soil crust organisms.

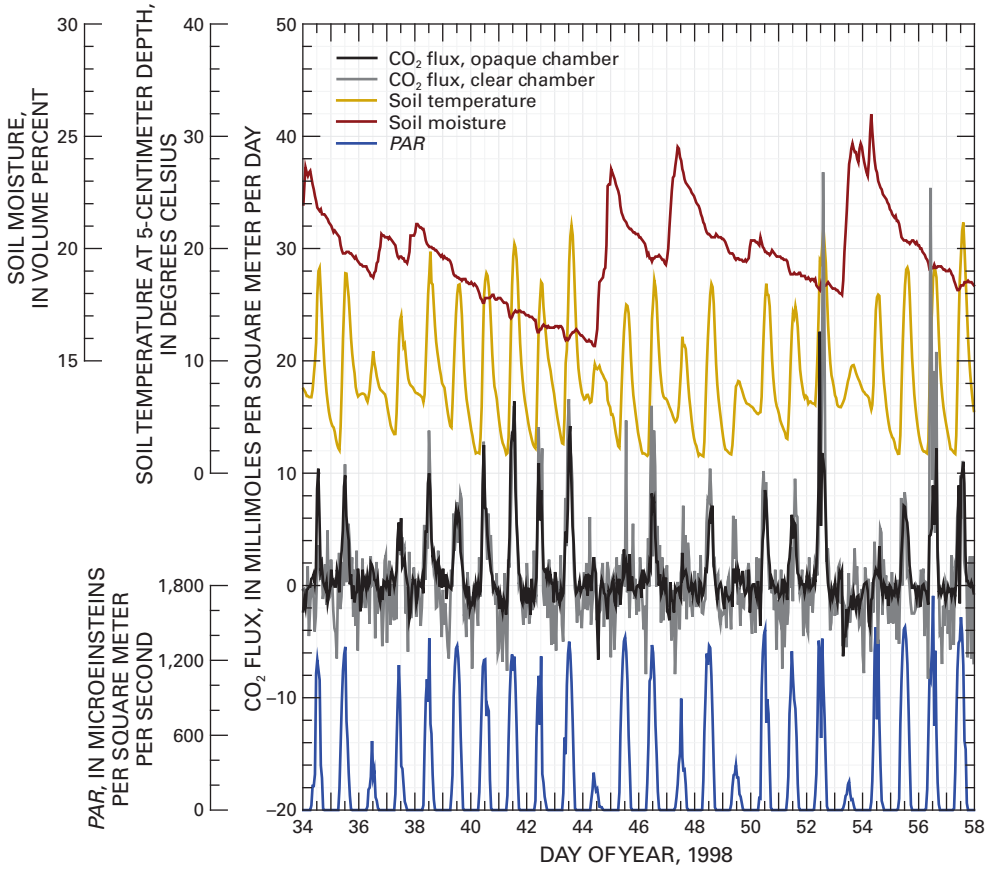

Figure 12. Hourly CO_2 flux from cool moist soil, February 1998. The midday soil-moisture dips on days when the soil was warmest (for example, DOY 40–43) are thermal artifacts of the soil moisture probe.

Summary

Fluxes from cool moist soils tended to be controlled primarily by soil temperature, except after rains when there were often small downward fluxes. The post-rain down-fluxes were apparently caused by soil calcite dissolving into infiltrating rainwater, which sharply increased CO_2 solubility. Fluxes, particularly opaque-chamber fluxes, were larger from cool moist soil than from cool dry soil, indicating that the moisture stimulated increased CO_{2biol} production despite the low temperature.

Fluxes from Hot Dry Soil

This discussion of fluxes from hot dry soil is based on an ensemble of 53 cloudless days from June, July, and August 1998 and 1999. Ensemble mean daily soil temperature at 5-cm depth was 38.0°C; mean daily temperatures of the days making up the ensemble ranged from 32.2° to 43.3°C. Ensemble mean daily soil moisture was 6.0 percent (table 2); mean daily soil moistures recorded during the ensemble ranged from 5.5 to 7.0 percent. The following sections introduce unusual features of flux that provide clues important to identifying and quantifying the CO_2 sources and physicochemical mechanisms that shaped the daily progression of fluxes from hot dry soil.

Peak Up-Fluxes from 9:00 to 10:00

Richter (1972) and Risk and others (2002) report that the timing of CO_2 fluxes from soils does not necessarily follow the timing of CO_{2biol} production in them, and that changing temperature can directly control CO_2 fluxes without regard to temperature's effect on CO_{2biol} production. A similar disjunction between CO_{2biol} production and CO_2 flux occurred in hot dry Amargosa Desert soil. The atmospheric-humidity boundary condition at the soil surface dictates that the top few centimeters of the soil must have been very dry during the day, effectively inhibiting CO_{2biol} production. In the interval between the dry top few centimeters of the soil and 25 cm deep, increased soil moisture may have supported minor metabolic activity; however, increased metabolic CO_2 production due to rising temperature in that interval cannot have been

the source of the morning flux peak because surface release of CO_{2biol} produced in that interval would lag temperature increase, and even as shallow as 5 cm deep, soil temperature did not peak until 4.5 hrs after the morning flux peak (fig. 13). Below 25 cm, daily soil moisture and temperature variation were small, so CO_{2biol} production below 25 cm should have been virtually constant. Hence, the morning up-flux peak cannot have been directly caused by CO_{2biol} production.

Clear-Chamber Fluxes 2.2 Times as Large as Opaque-Chamber Fluxes

Because clear- and opaque-chamber fluxes should be the same in the absence of photosynthesis, clear-chamber daily fluxes 2.2 times as large as opaque-chamber daily fluxes from hot dry soils (table 2) is a surprise. At night, when the difference in their optical transmissivities was inconsequential to conditions inside the chambers, the two chambers (both had short lids) measured fluxes that were similar, indicating that the difference is unlikely to have been due to instrumental measurement bias or mechanical differences (figs. 13, 14). Matthias and Peralta Hernàndez (1998) report that when an opaque chamber is installed on dry soil at midday, near-surface soil temperature tends to drop. Under the same conditions, a clear chamber lid, which transmits 80–90 percent of the up to about 1,200 watts m^{-2} of downwelling solar radiation to the soil surface, probably artificially increases soil surface temperature by the greenhouse effect and inhibiting convective heat loss. Stimulation of daytime CO_2 up-flux by solar heating also is consistent with the occurrence of smaller flux peaks on cloudy days (such as DOY 209 in fig. 14) when insolation and hence soil heating were much reduced. Furthermore, the flux difference developed in the 4 minutes the lids were down for a measurement; this indicates that a substantial part of the flux originated very near the soil surface, because changes in solar heating cannot propagate very far into the soil in such a short time. From these considerations, it appears that the natural daytime flux is probably intermediate between the clear- and opaque-chamber fluxes. Therefore, the different total daily fluxes measured by the clear and opaque chambers appears to be a flux-chamber artifact that highlights the role of near-surface temperature changes in regulating release of soil CO_2 to the atmosphere.

Rain-Induced Up-Flux Spikes

Unlike cool moist soil, where up-flux was stanched by rainfall, rains on hot dry soil elicited abrupt, tall flux spikes (figs. 7, 8, 15). The spikes occurred without regard for the time of day and usually lasted an hour or two. The tallest spikes were the largest fluxes measured during the study. After spiking, flux decreased quickly to about half to two-thirds of the spike height, then declined to pre-rain levels over the course of a week or two (fig. 15). Contrary to the hot-dry-soil norm where clear-chamber daily fluxes were more than double opaque-chamber fluxes, rain-induced opaque-chamber flux spikes were typically about twice the height of clear-chamber flux spikes. When two rains fell a few days apart, the flux spike caused by the second rain typically was distinctly shorter than the flux spike caused by the first rain, even though soil moisture was generally greatest during the second rain.

Note that Parkin and Kaspar (2004) observed rain-induced up-flux spikes in their study of CO_2 fluxes from a no-till corn and soybean plot in Boone County, Iowa, and they cite four other papers that also report flux increases in response to rain. The flux spikes observed by Parkin and Kaspar resemble the Amargosa Desert flux spikes in that there is no apparent strong correlation between the amount of rainfall and the size of the flux increase. However, the Iowa flux increases arose from soil with >18 percent volumetric water content, whereas the Amargosa Desert flux responses arose from soil with <8 percent volumetric water content. No such flux responses occurred from Amargosa Desert soils having >12 percent volumetric water content, which suggests that different CO_2 release mechanisms operate in the two environments.

Nocturnal Down-Fluxes

The nocturnal down-fluxes in figures 13 and 16 are likely to be of physicochemical origin because photosynthesis, the primary biological process that consumes CO_2, normally does not operate at night or on bare dry soils. Because upward CO_{2gw} diffusion from the water table (Prudic and Striegl, 1994) and CO_{2biol} production at depth continue through the night, the CO_2 gradient at depth is always upward. The simultaneous up-fluxes from depth and nocturnal down-fluxes at the surface require a CO_2 reservoir near the soil surface that fills at night and empties during the day.

CO_2 Reservoir Mechanisms

Knowledge of the mechanism(s) responsible for the soil's near-surface CO_2 reservoir and their behavior is key to understanding the unusual flux responses of hot dry soil. In the following paragraphs, six possible reservoir mechanisms are evaluated for their ability to account for the magnitude and timing of nocturnal down-fluxes: (1) barometric pumping, (2) thermal pumping, (3) down-advection of air caused by condensation of water in the soil, (4) dissolution of CO_2 into condensing soil water, (5) CO_2 dissolution into/exsolution from soil water in response to temperature change (thermal solubility), and (6) CO_2 adsorption onto/desorption from soil mineral grains in response to temperature change (thermal sorption).

Barometric pumping, thermal pumping, and down-advection of air in response to reduction in soil-gas volume caused by the condensation of soil moisture can all move small amounts of air into soil at night. However, these processes cannot have been responsible for the measured nocturnal CO_2 down-flux because movement of air into the soil does not cause the chamber headspace CO_2 concentration changes from which CO_2 fluxes are calculated. Hence, although small CO_2 fluxes were probably associated with these processes, none was a primary CO_2-reservoir mechanism.

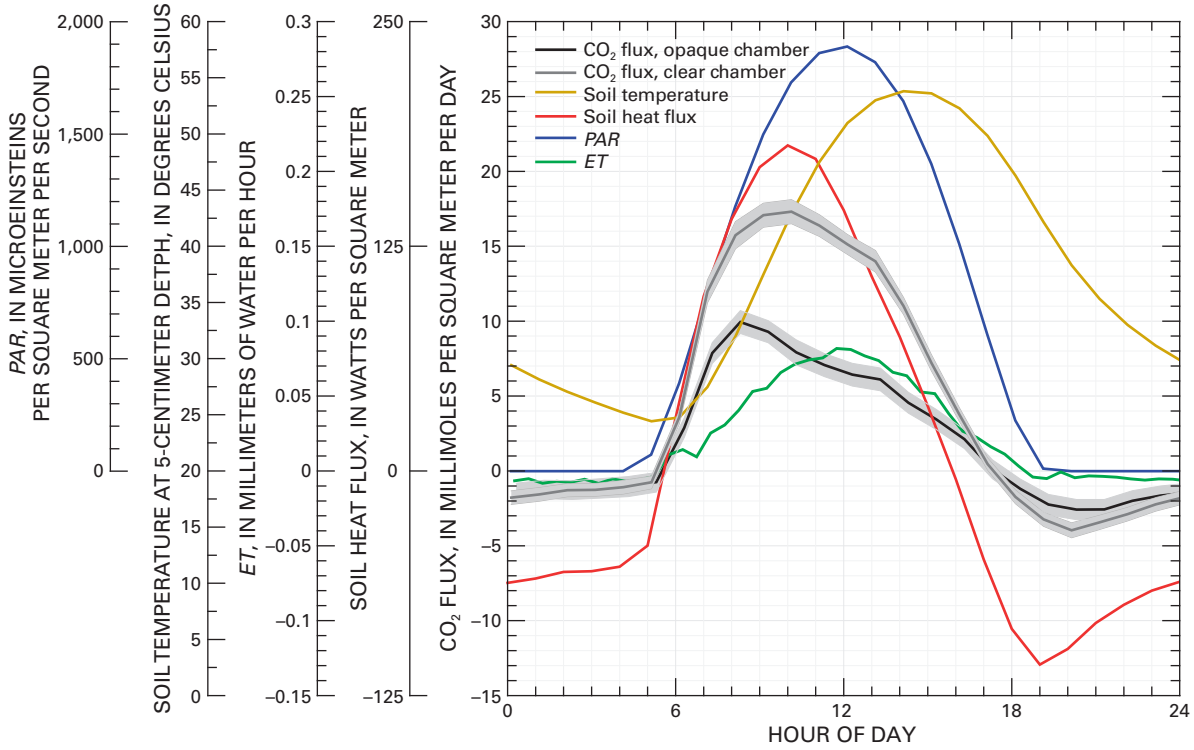

Figure 13. Ensemble fluxes, soil temperature and moisture, photosynthetically active radiation (*PAR*), and evapotranspiration (*ET*) from hot dry soil. The light gray band surrounding the CO_2-flux curves is the 2-σ uncertainty envelope. Plotted at the same scale as the warm moist soil ensemble (fig. 11).

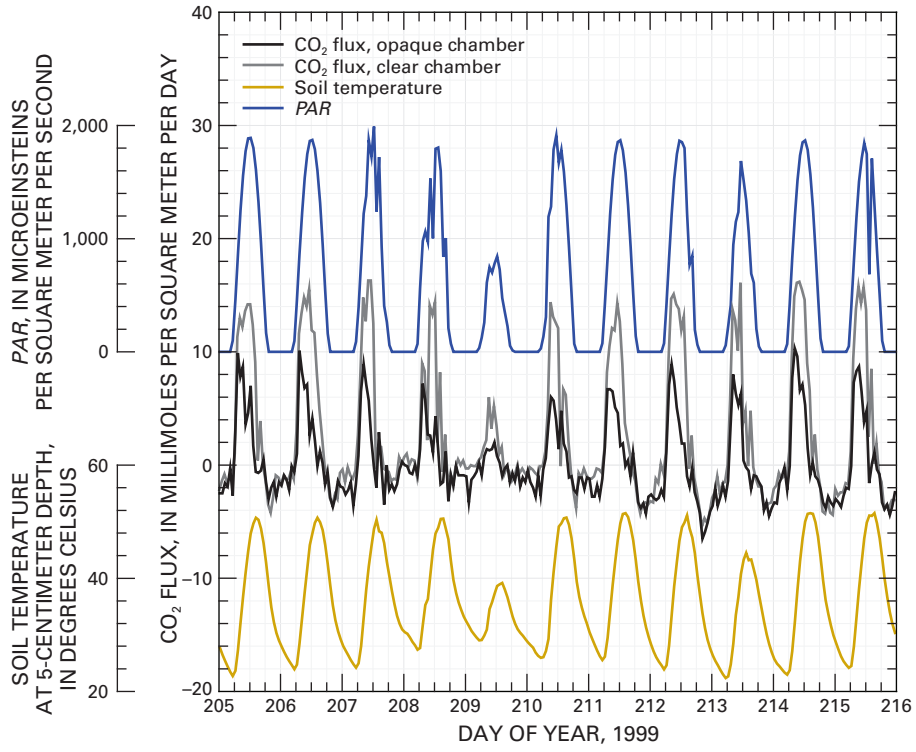

Figure 14. Hourly record showing solar radiation's control, by way of its proxy, photosynthetically active radiation (*PAR*), on variations in CO_2 flux and soil temperature. See also figure 15.

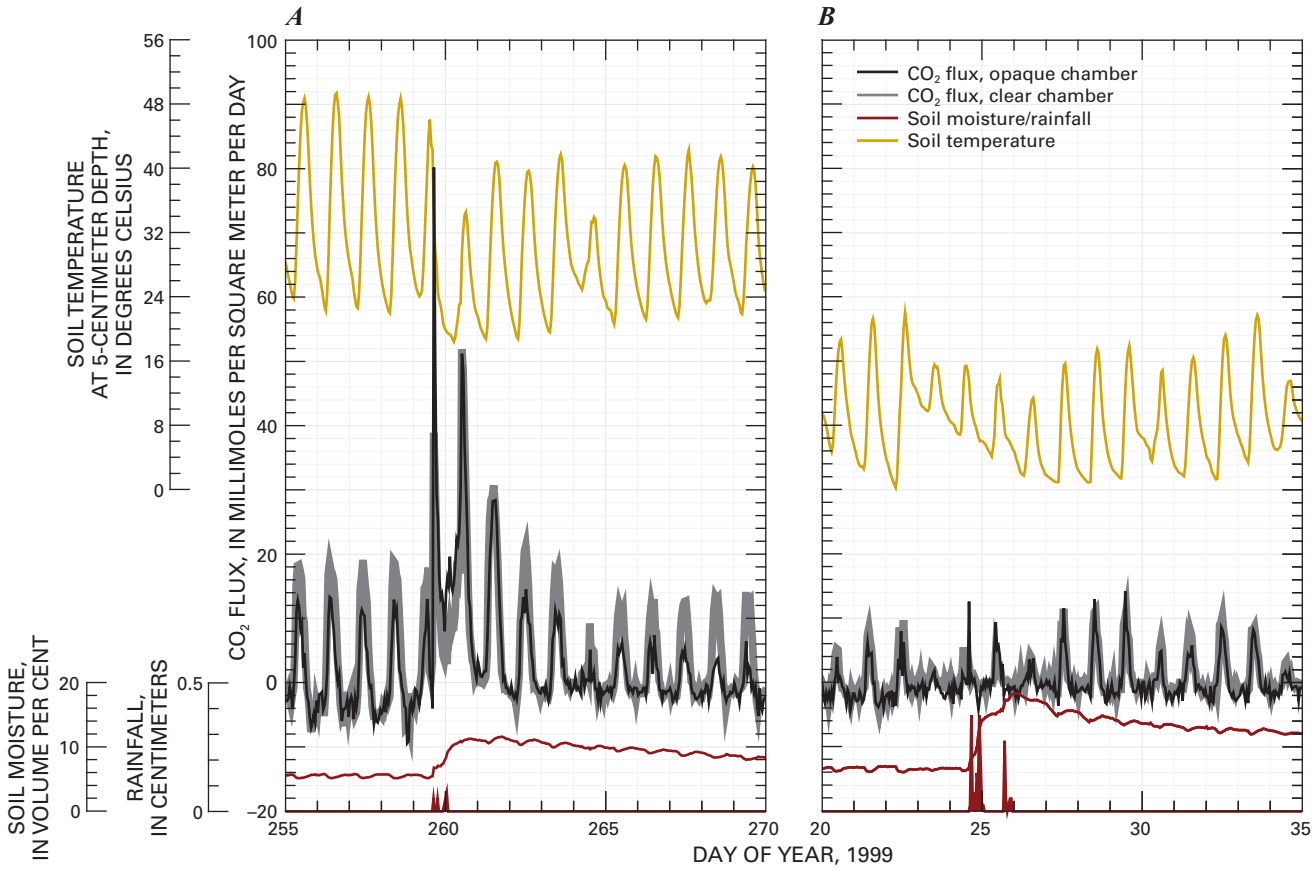

Figure 15. Two sections of record demonstrating the variable temperature dependence of CO_2 flux on rainfall. *A*, Hot dry soil. *B*, Cool dry soil.

Dissolution of CO_{2air} into nocturnal condensation is quantitatively incapable of accounting for the nocturnal down-flux. Assuming a soil temperature of 20°C, a CO_2 partial pressure of $10^{-3.0}$ atm, nocturnal condensation (downward *ET*) of 63 mL m^{-2} (table 2), and enough calcite in the soil to buffer the dissolution of CO_2 in soil water, PHREEQC indicates that a maximum of 0.05 mmol m^{-2} of CO_2 could dissolve into soil water during the night. That amount is <7 percent of the 0.8 and 1.1 mmol CO_{2air} m^{-2} nocturnal down-flux in the opaque and clear chambers, respectively.

The maximum fluxes induced by thermal solubility can be estimated as the product of the volume of soil water and the change in CO_2 solubility between maximum and minimum soil temperatures. Maximum and minimum temperatures at 5-cm depth were 54°C and 24°C (fig. 13), with respective CO_2 solubilities (calculated by PHREEQC) of 0.46 mmol L^{-1} and 0.76 mmol L^{-1}, assuming a P_{CO_2} of $10^{-3.0}$ atm and equilibrium with calcite. The 0.30 mmol L^{-1} difference between the solubilities times the 6 L m^{-2} of water in the top 10 cm of the soil (6 percent soil moisture × 100 L of soil) yields 1.8 mmol of CO_2 m^{-2}, the maximum that could dissolve as the soil cooled at night or exsolve as soil warms during the day, or about twice the observed nocturnal CO_2 down-flux (table 2). Hence, the thermal solubility of CO_2 in soil water is quantitatively capable of being the CO_2-reservoir mechanism.

Thermal sorption is the final mechanism that could be responsible for the soil's CO_2-reservoir behavior. Figure 6 shows that the upper 3–4 mm of dry Amargosa Desert soil can adsorb an amount of CO_2 equivalent to the total nocturnal CO_2 down-flux (0.8 and 1.1 mmol m^{-2}, opaque and clear chambers, respectively) in response to a temperature decrease from 63.7° to 12.3°C (fig. 6), the maximum and minimum soil surface temperatures of the hot dry ensemble (calculated using the equations in Campbell, 1977, a soil thermal diffusivity of 0.3 square millimeters per second (mm^2 s^{-1}) estimated from fig. 2.7 in Campbell, 1977, and the maximum and minimum temperatures at 5-cm depth). How the laboratory results relate to the actual CO_2 adsorption/desorption in Amargosa Desert soils is an open question, primarily because of the potential for interactions with water, which is far more abundant than CO_2 in both air and soil, and which, by virtue of its dipole moment, is a better competitor than CO_2 for the sorption sites on soil mineral surfaces.

Because of the low-atmospheric-humidity boundary condition, the thin surface layer of the soil that could respond to changed conditions in the 4 minutes the chamber lids were down was even drier than the ensemble soil water content. Soil in the thin surface layer was so dry that most, if not all of the water was bound water (adsorbed or vicinal water) rather than bulk water (E. Weeks, U.S. Geological Survey, personal commun., 2006). Bound water has very different physicochemical characteristics than bulk water (Drost-Hansen, 1991). How the

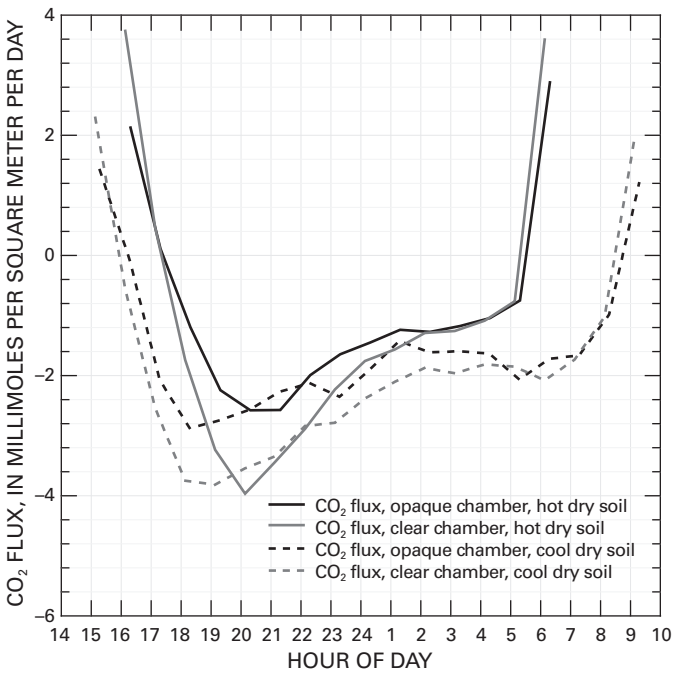

Figure 16. Ensemble nocturnal down-fluxes of CO_{2air} into hot dry and cool dry soils.

sorption sites on soil mineral grains were partitioned between bound water and CO_2, the extent to which CO_2 adsorbed on bound water, and the temperature dependence of those reactions are apparently unknown, so there is no way to estimate directly how much of the CO_2-reservoir behavior of the surface soil was due to thermal sorption. However, the following points indicate that actual thermal solubility probably was smaller than its calculated potential and that thermal sorption was probably an important, possibly the primary, CO_2-reservoir mechanism in hot dry soil.

- Although the data are irregularly variable, there was an unambiguous tendency for the largest nocturnal down-fluxes to occur when the soil was driest. The size of nocturnal down-fluxes was unrelated to temperature (fig. 17).
- Clear- and opaque-chamber daily peak CO_2 up-fluxes preceded the daily *ET* peak by 2 and 3 hrs, and the daily soil heat flux peak (a measure of soil temperature change) by a few minutes and an hour and a quarter, respectively (fig. 13). These temporal relations indicate that the CO_2 reservoir was located very near the soil surface where the soil was driest.
- The tall abrupt up-flux spikes that occurred in the first 5 hrs after the beginning of rains on hot dry soil (fig. 15) suggest rapid releases from a CO_2 reservoir; Stevenson (1956) and Funke and Harris (1968) found that biological CO_2 production takes 6–8 hrs to ramp up after dry soils are rewetted. Similarly, the flux spikes could not have been caused by release from a thermal solubility reservoir because adding water to an aqueous reservoir should increase its capacity. The total fluxes for the first 5 hrs after three rains on hot dry soil (DOY 241–242, 1998; DOY 189 and 259, 1999; see figs. 7, 8) ranged from 8.3 to 11.6 mmol CO_2 m^{-2}. According to figure 6, on those days about 0.4 mmol CO_2 could have adsorbed onto a volume of critically dry soil 1 m^2 by 1 mm deep. To the extent that in-place soil had the same sorptive capacity as critically dry soil, displacement of adsorbed CO_2 from a 2- to 3-cm-deep layer of soil could account for the initial flux spikes.
- The correlation coefficients between soil heat flux and the CO_2 fluxes from both chambers are 0.98, whereas the correlation coefficients between *ET* and clear- and opaque-chamber CO_2 fluxes are 0.94 and 0.89, indicating direct temperature control on CO_2 flux.
- At times CO_2 flux and *ET* were in opposite directions.

These points suggest that near-soil-surface thermal sorption of CO_2 was the primary CO_2-reservoir mechanism, though thermal solubility may have been an important contributor to ensemble flux at certain times of day. Note that Obrist and others (2003) observed nocturnal CO_2 down-fluxes in both native sagebrush and post-fire successional communities in northwest Nevada. Also, one of the CO_2 sorption values that Striegl and Armstrong (1990) measured on wet and dry soils from Illinois was very similar to that of Amargosa Desert soil, and Walvoord and others (2005) invoke CO_2 adsorption in the deep unsaturated zone in the Amargosa Desert to improve model results.

Movements of CO_2 into and out of the soil may be enhanced by the thermal effusion of CO_2, as described by Turlyun (1958). According to Turlyun, when the passage width between the soil grains is less than the mean free path of the soil gas molecules, temperature gradients can induce migration of CO_2 molecules towards the warmer end of the gradient several orders of magnitude faster than ordinary diffusive flux. This process is probably not a significant contributor to fluxes from the relatively coarse Amargosa Desert soils, but it could be important in other environments.

CO_2 Sources

Three different CO_2 sources contributed to the daytime up-flux: CO_{2biol}, CO_{2gw}, and CO_{2air}. The night-time down-flux was composed entirely of CO_{2air} (fig. 18). An important consequence of the CO_2-reservoir behavior of the soil is that CO_2 was released to the atmosphere in daily pulses, even though CO_{2gw} was delivered from depth at a constant rate, CO_{2biol} was continuously if somewhat cyclically produced, and CO_{2air} was continuously available. Of the 5.6 mmol m^{-2} d^{-1} total daytime clear-chamber up-flux, 4.2 mmol m^{-2} d^{-1} (75 percent) was CO_{2biol}, 1.1 mmol m^{-2} d^{-1} (20 percent) was recycled CO_{2air}, and 0.3 mmol m^{-2} d^{-1} (5 percent) was CO_{2gw} (table 2). Opaque-chamber fluxes were similarly partitioned, with the 2.8 mmol m^{-2} d^{-1} total daytime up-flux comprising 1.7 mmol m^{-2} d^{-1} (61 percent) CO_{2biol}, 0.8 mmol m^{-2} d^{-1} (29 percent) recycled CO_{2air}, and 0.3 mmol m^{-2} d^{-1} (11 percent) CO_{2gw} (table 2). The difference between clear- and opaque-chamber fluxes is, as discussed above, primarily an artifact of the substantially

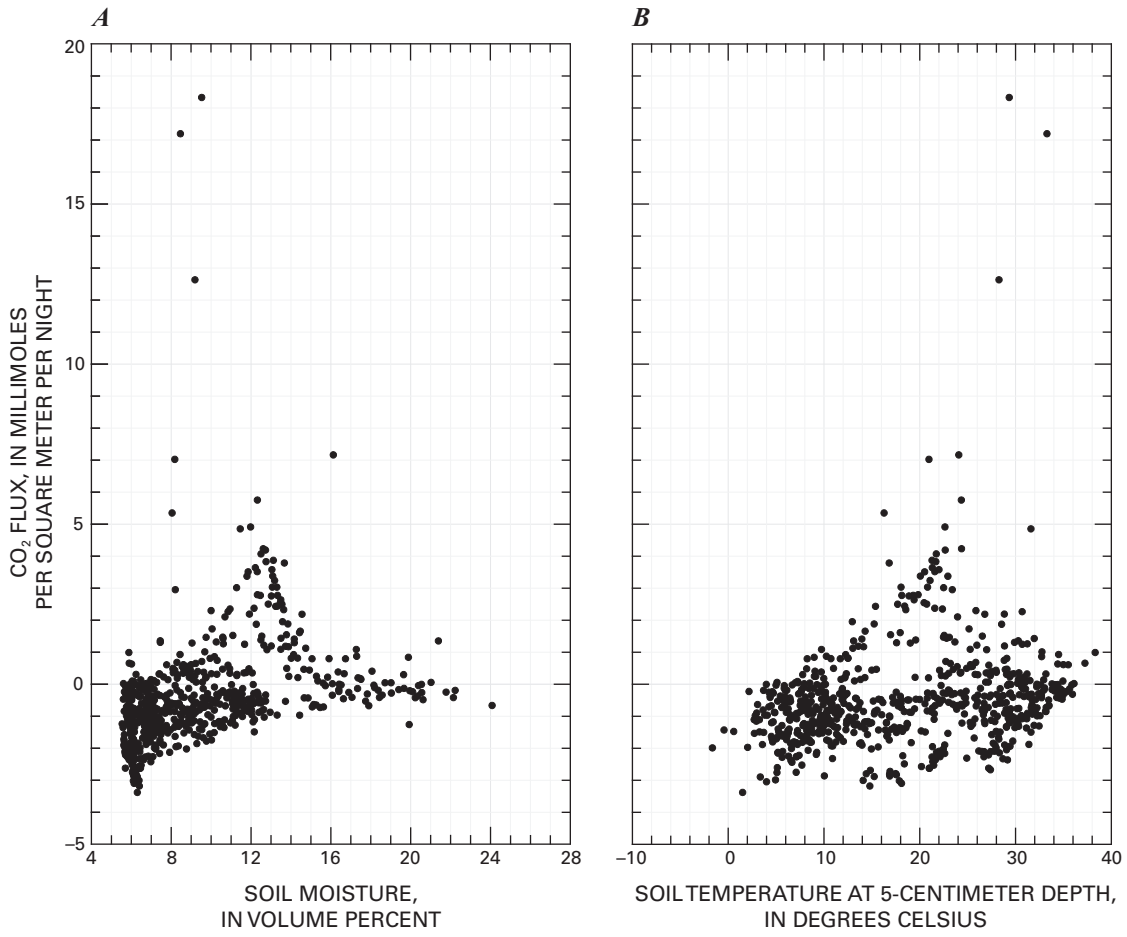

Figure 17. Total nocturnal (*PAR* = 0) opaque-chamber fluxes from the 697 nights with uninterrupted data recovery plotted against soil moisture (*A*) and temperature (*B*). The up-flux peak (centered around a soil moisture of about 13 percent) in figure 17*A* marks active nocturnal CO_{2biol} production in warm moist soil in the spring of 1998 (see also fig. 11). Fluxes decreased as the soil dried.

different conditions in the two chambers during the 4 minutes each hour when the lids were down during daylight hours. What is less apparent is that the smaller opaque-chamber nocturnal down-flux is probably also a consequence of the daytime differences between the fluxes from the two chambers, because the opaque chamber, having had its CO_2 reservoir drawn down less during the day, required less CO_2 uptake to top it off at night. The control that the CO_2 reservoir exerts on CO_2 fluxes is presented diagrammatically in figure 18. When the reservoir is below capacity, primarily as a consequence of soil cooling, the reservoir layer at the soil surface intercepts all CO_{2gw} and CO_{2biol} diffusing up from below, as well as scavenging CO_{2air} from the atmosphere (fig. 18*A*). When soil warming causes reservoir capacity to shrink below the amount of CO_2 in storage, the reservoir starts to vent CO_2 (the soil-surface up-arrow in figure 18*B* marked CO_{2air}, CO_{2biol}, CO_{2gw}), and the net flux of CO_{2air} into the soil goes to zero. As the soil warms below the depth of the reservoir layer, the reservoir continues venting CO_2, and CO_{2biol} and CO_{2gw} from below the reservoir layer are transmitted to the atmosphere unimpeded. The upward flux of CO_{2biol} from the above-ground part of the plant denotes the release of metabolic CO_2 produced by the non-photosynthetic parts of the plant (fig. 18*B*).

Summary

As would be expected, CO_2 fluxes from hot dry soil were small. What was unexpected was the presence of a near-surface CO_2 reservoir, probably based on thermal sorption or a combination of thermal sorption and thermal solubility, whose capacity was an inverse function of soil temperature. The presence of the reservoir emphasizes that temperature, in addition to controlling CO_{2biol} production, directly controls the transport of CO_2 across the soil-air interface. Carbon-dioxide-reservoir behavior caused fluxes from hot dry soil to mimic the daily soil-heat-flux pattern much more closely than the CO_{2biol}-production pattern, including nocturnal down-fluxes and mid-morning peak up-fluxes. From this, it is apparent that measurements of CO_2 fluxes from soils with well developed CO_2-reservoir behavior will be fraught with artifacts, given that all chambers, particularly opaque chambers, strongly perturb the input and redistribution of solar energy.

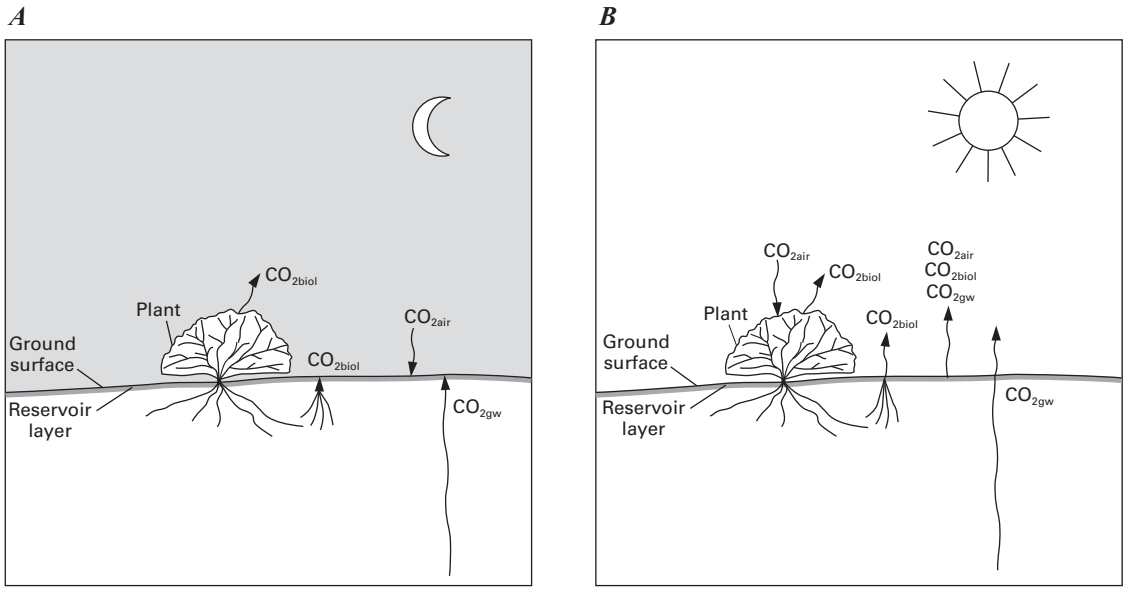

Figure 18. Schematic showing how the CO_2 reservoir behavior of dry soil impacts CO_2 fluxes when the reservoir is below capacity (*A*) and at or above capacity (*B*).

Fluxes from Cool Dry Soil

This discussion of fluxes from cool dry soil is based on an ensemble (fig. 19, table 2) of 36 cloudless cool-season days. Ensemble mean soil temperature (5-cm depth) was 9.3°C, with mean temperature of the individual days ranging from 2.2° to 14.9°C. Ensemble mean volumetric soil moisture in the top 10 cm of the soil was 6.8 percent, with mean soil moisture of the individual days ranging from 6.5 to 7.3 percent. The progression of fluxes from cool dry soil resembles the progression of fluxes from hot dry soil (figs. 13, 19), in that daytime fluxes were upward, peaking at or before noon; nocturnal fluxes were downward; daily clear-chamber fluxes exceeded opaque-chamber fluxes by more than a factor of two; the sequence of afternoon flux reversals was the same in both, with soil heat flux reversing first, followed 1.5 hrs later by CO_2 flux reversal, followed 1–1.5 hrs later by *ET* reversal; and on overcast days daytime up-fluxes were small. Important differences between the daily flux progressions from cool dry and hot dry soils and the mechanisms that might be responsible for them are discussed in the following four sections.

Small Fluxes on Cool Dry Days

Cool dry soils produced by far the smallest fluxes of any of the sets of conditions (table 2). Nocturnal CO_2 down-fluxes equaled 81 percent and 93 percent of the daytime clear- and opaque-chamber up-fluxes (fig. 19, table 2), hence the vast majority of daytime up-flux was recycled CO_{2air}. Furthermore, Thorstenson and Prudic's (U.S. Geological Survey, unpub. data, 2002) modeled CO_{2gw} up-flux of 0.3 mmol m^{-2} d^{-1} (± a factor of 2) is indistinguishable from the 0.4 and 0.1 mmol m^{-2} d^{-1} mean daily fluxes measured by the clear and opaque chambers, when the uncertainty in both modeled and measured fluxes is taken into account, and considering that clear- and opaque-chamber fluxes probably bracket the real flux. Therefore, fluxes from cool dry soil were almost exclusively of physical origin.

Lagged Morning Flux Reversal

Morning CO_2 flux reversal from cool dry soil lagged the morning soil-heat-flux reversal by at least an hour, instead of the nearly concurrent reversal observed on hot dry soil (figs. 13, 19, table 2). If the nearly simultaneous reversal of soil heat flux and soil CO_2 flux from hot dry soil is an indication that the CO_2 reservoir was nearly full by morning, then the lagged cool-dry-soil CO_2 flux reversal (fig. 19) indicates that the cool dry soil CO_2 reservoir was substantially below capacity when the soil warming began. The reservoir fell short of filling during the night partly because of the negligible CO_{2biol} production in cool dry soil and partly because the reservoir capacity of cool dry soil was about 8 times as large as the reservoir capacity of hot dry soil (assuming that reservoir capacity scales with temperature as shown in figure 6, and that the calculated 2.2°–16.4°C and 18.0°–59.8°C soil-surface-temperature ranges of cool and hot dry soils are substantially correct). The progression of nocturnal down-fluxes also is consistent with a cool dry soil reservoir that was below capacity, in that down-fluxes into hot dry soil decreased through the night, whereas nocturnal down-fluxes into cool dry soil decreased until hour of day 1:00–2:00 then stabilized, or even increased slightly, until morning heating caused the reservoir to shrink and flux to reverse direction (fig. 15).

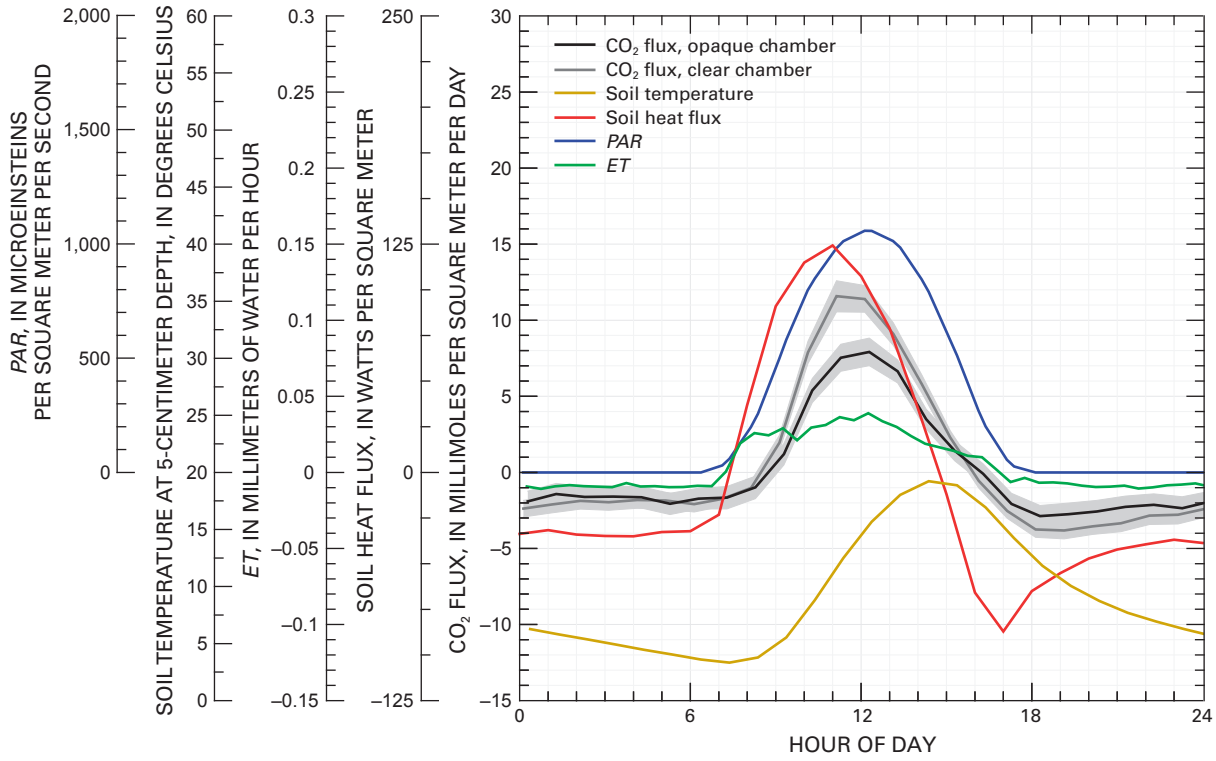

Figure 19. Ensemble CO_2 fluxes and other physical variables from cool dry soil. The light grey band surrounding the CO_2-flux curves is the 2-σ uncertainty envelope. Plotted at the same scale as the warm moist soil ensemble (fig. 11) and the hot dry soil ensemble (fig. 13).

Lagged Midday Flux Peak

Peak CO_2 up-flux from cool dry soil occurred nearly concurrently with peak *ET* and *PAR* and lagged peak soil heat flux by an hour or more, rather than leading *ET* and *PAR* and occurring about concurrently with soil heat flux, as was the case in hot dry soil (figs. 13, 19). The near concurrence of the flux and *ET* peaks and a correlation coefficient between CO_2 flux and *ET* (0.89 clear and opaque chambers) larger than that between CO_2 flux and soil heat flux (0.84 clear chamber, 0.83 opaque chamber) both suggest that CO_2-water interactions may have been more important in CO_2 fluxes from cool dry soil than from hot dry soil. However, CO_2 release as soil water evaporated cannot be the primary mechanism contributing to daytime CO_2 up-flux. According to PHREEQC, the 225 mL m^{-2} of water lost to *ET* during the cool-dry-soil ensemble day (fig. 19, table 2) could have dissolved 0.24 mmol of CO_2 m^{-2}, assuming soil P_{CO_2} was $10^{-3.0}$ atm, soil temperature was 5°C, and the water was in equilibrium with calcite. The daytime clear- and opaque-chamber CO_2 up-fluxes were 2.1 mmol m^{-2} and 1.4 mmol m^{-2}, or 8.8 and 5.8 times the amount of CO_2 that could be released as soil water evaporated, assuming *ET* was all *E*. Potential daily thermal solubility is estimated as the product of 0.27 mmol L^{-1} (the difference in CO_2 solubility in bulk water in equilibrium with calcite between the 3.0°C minimum and 19°C maximum temperatures at 5-cm depth) and 6.8 l m^{-2} (the volume of water in the upper 10 cm of the soil), or 1.9 mmol m^{-2}. Hence, potential thermal solubility variations are roughly equivalent to the daily up- and down-fluxes in cool dry soil (table 2). Actual thermal solubility fluxes were probably smaller than the calculated potential because bulk water was concentrated at depths where response to surface temperature inputs was lagged and muted (note how soil temperature at 5-cm depth lags CO_2 flux in fig. 19). This suggests that a substantial portion of the CO_2 fluxes was due to near-surface thermal sorption onto bare mineral surfaces and (or) bound water. Hence, thermal sorption, thermal solubility, and incomplete CO_2-reservoir filling all may have contributed to retarding peak CO_2 fluxes from cool dry soil.

Flux Response to Rainfall

Decreased clear-chamber flux and the small opaque-chamber flux spike caused by the one rainfall on cool dry soil are quite different responses than the large up-flux spikes that rain elicited from hot dry soil (fig. 15). The different responses were not due to pre-rain differences in soil moisture (fig. 15). Similarly, the small fluxes at the onset of the rains indicate that both CO_2 reservoirs were close to capacity (figs. 15, 6). This indicates that there was a fundamental difference in the character of hot-soil and cool-soil CO_2 reservoirs. Given that

a CO_2 reservoir based on binding with bulk or bound water should not release CO_2 when more water is added, it is tempting to attribute the cool-dry-soil response to rainfall as that of a CO_2-water reservoir. But until the vertical distribution of bulk and bound water and the temperature dependence of their interactions with CO_2 are better characterized, the exact mechanism(s) responsible for the different flux responses to rain will remain a mystery.

Summary

The daily pattern of CO_2 fluxes from cool dry soil was similar to the pattern of fluxes from hot dry soil, but net daily fluxes from cool soil were less than a tenth of hot-soil fluxes because CO_{2biol} production in cool dry soil was undetectable. Most of the CO_2 released from the soil was recycled CO_{2air}. Lacking substantial contributions of CO_{2biol}, the down-flux of CO_{2air} was too slow to fill the reservoir during the night, so down-flux into the reservoir continued for one and a half hours in the morning after *ET* and soil heat flux had reversed direction. The minimal flux response to rainfall and the concurrent midday CO_2 flux and *ET* peaks from cool dry soil indicate that water is likely to have played a larger role in the cool-dry-soil CO_2 reservoir than it did in the hot-dry-soil reservoir. To fully understand the CO_2 reservoir behavior of cool dry soil, the temperature dependence of the soil's uptake and release of CO_2 and H_2O and the interactions between H_2O and CO_2 need to be quantified.

Conclusions

A long-term record of soil CO_2 flux and related physical variables provides a good basis for evaluating the identity, size, and timing of the various biophysicochemical mechanisms that make substantial contributions to soil CO_2 flux. In the Amargosa Desert, daily fluxes were small and their sizes scaled with suitability of soil conditions for CO_{2biol} production, with the largest continuous fluxes emanating from warm moist soil, and the smallest from cool dry soil. However, hourly fluxes were controlled primarily by the uptake and release of CO_2 by solubility and sorption reservoirs in the soil. Carbon-dioxide-reservoir capacity was an inverse function of temperature, so the reservoirs tended to take up CO_{2biol}, CO_{2gw}, and CO_{2air} as the soil cooled at night and release roughly equivalent amounts of CO_2 as the soil warmed during the day, hence the CO_2 reservoirs tended to have little impact on total daily fluxes. Carbon dioxide reservoirs have two important implications for chamber measurement of fluxes. First, because the dry-soil reservoir captured and stored CO_2 at night and then released it the following day, measuring flux only during daylight hours, as is often done with manual chambers, necessarily introduces large errors. Second, because all chambers, particularly opaque ones, disturb the natural temperature regime, chamber measurement of fluxes from soils having large CO_2 reservoirs are subject to unavoidable artifacts.

In summary, the transfer of CO_2 between the soil and the atmosphere is a complex process; to truly understand it requires a good understanding of the near-soil-surface interactions between CO_2, bulk and bound water, and soil particles. In particular, the apparent lack of information on the nature and magnitude of CO_2's interaction(s) with bound water limits our ability to fully understand CO_2's near-soil-surface behavior. Furthermore, it is unlikely that the Amargosa Desert CO_2 reservoirs are the only mechanisms that cause the flux pattern to deviate from the pattern of CO_{2biol} production and diffusive escape to the atmosphere. As the detailed structure of fluxes and other physical variables from other environments are characterized, additional mechanisms that modulate the timing and amount of flux are likely to be discovered.

Acknowledgments

The following people (in alphabetical order) made important contributions to field and laboratory work, data analysis, and discussions of the technical and philosophical underpinnings of soil CO_2 flux: Dean Anderson, Brian Andraski, Larry Beaver, Jayne Belnap, Cary Chiou, Bernadette Graham, Douglas Halm, Richard Healy, William Herkelrath, Mike Johnson, Jerry Leenheer, David Litke, Scott McFarlane, David Parkhurst, Niel Plummer, David Rutherford, Dwight Schmidt, Donald Thorstenson, Edwin Weeks, and John Whitney.

References Cited

Campbell, G.S., 1977, An introduction to environmental biophysics: New York, Heidelburg Science Library, Springer-Verlag, 159 p.

Davidson, E.A., Belk, E., and Boone, R.D., 1998, Soil water content and temperature as independent or confounded factors controlling soil respiration in a temperate mixed hardwood forest: Global Change Biology, v. 4, p. 217–227.

Drost-Hansen, W., 1991, Some effects of vicinal water on the sedimentation process, compaction, and ultimate properties of sediments, *in* Bennett, R.H., Bryant, W.R., and Hulbert, M.H., eds., Frontiers in sedimentary geology. Microstructure of fine-grained sediments—From mud to shale: New York, Springer-Verlag, p. 259–266.

Field, C.B., and Raupach, M.R., eds., 2004, The global carbon cycle—Integrating humans, climate, and the natural world: Washington, D.C., Island Press, 526 p.

Freundlich, H., 1926, Colloid and capillary chemistry [English translation of the 3d German edition]: London, Methuen, 883 p.

Fuchs, M., and Tanner, C.B., 1968, Calibration and field test of soil heat flux plates: Soil Science Society of America Proceedings, v. 32, p. 326–328.

Funke, B.R., and Harris, J.O., 1968, Early respiratory responses of soil treated by heat or drying: Plant and Soil, v. 28, p. 38–48.

Healy, R.W., Striegl, R.G., Russell, T.F., Hutchinson, G.L., and Livingston, G.P., 1996, Numerical evaluation of static-chamber measurements of soil-atmosphere gas exchange—Identification of physical processes: Soil Science Society of America Journal, v. 60, p. 740–747.

Janssens, I.A., Kowalski, A.S., Longdoz, B., and Ceulemans, R., 2000, Assessing forest soil CO_2 efflux—An in situ comparison of four techniques: Tree Physiology, v. 20, p. 23–32.

Johnson, M.J., Mayers, C.J., and Andraski, B.J., 2002, Selected micrometeorological and soil-moisture data at Amargosa Desert Research site in Nye County near Beatty, Nevada, 1998–2000: U. S. Geological Survey Open-File Report 02–348, 21 p.

Matthias, A.D., and Peralta Hernàndez, A.R., 1998, Modeling temperatures in soil under an opaque cylindrical enclosure: Agricultural and Forest Meteorology, v. 90, p. 27–38.

Nay, S.M., Mattson, K.G., and Bormann, B.T., 1994, Biases of chamber methods for measuring soil CO_2 efflux demonstrated with a laboratory apparatus: Ecology, v. 75, p. 2,460–2,463.

Nichols, W.D., 1987, Geohydrology of the unsaturated zone at the burial site for low-level radioactive waste near Beatty, Nye County, Nevada: U.S. Geological Survey Water-Supply Paper 2312, 57 p.

Obrist, D., Delucia, E.H., and Arnone, J.A., III, 2003, Consequences of wildfire on ecosystem CO_2 and water vapor fluxes in the Great Basin: Global Change Biology, v. 9, p. 563–574.

Parkhurst, D.L., and Appelo, C.A.J., 1999, User's guide to PHREEQC (version 2)—A computer program for speciation, batch reaction, one-dimensional transport, and inverse geochemical calculations: U.S. Geological Survey Water Resources Investigations Report 99–4259, 312 p.

Parkin, T.B., and Kaspar, T.C., 2004, Temporal variability of soil carbon dioxide flux—Effect of sampling frequency on cumulative carbon loss estimation: Soil Science Society of America Journal, v. 68, p. 1,234–1,241.

Prudic, D.E. and Striegl, R.G., 1994, Water and carbon dioxide movement through unsaturated alluvium near an arid disposal site for low-level radioactive waste near Beatty, Nevada [abs.]: Eos, Transactions, American Geophysical Union, v. 75, no. 16, p. 161.

Raich, J.W., and Schlesinger, W.H., 1992, The global carbon dioxide flux in soil respiration and its relationship to vegetation and climate: Tellus B, v. 44, p. 81–99.

Richter, J., 1972, Evidence for significance of other-than-normal diffusion transport in soil gas Exchange: Geoderma, v. 8, p. 95–100.

Riggs, A.C., Striegl, R.G., and Maestas, F.B., 1999, Soil respiration at the Amargosa Desert research site, *in* Morganwalp, D.W., and Buxton, H.T., eds., U.S. Geological Survey Toxic Substances Hydrology Program—Proceedings of the technical meeting, Charleston, South Carolina, March 8–12, 1999 (v. 3): U.S. Geological Survey Water-Resources Investigations Report 99–4018C, p. 491–497.

Risk, D., Kellman, L., and Beltrami, H., 2002, Carbon dioxide in soil profiles—Production and temperature dependence: Geophysical Research Letters, v. 29, p. 11–1—11–4.

Rochette, P., and Hutchinson, G.L., 2005, Measurements of soil respiration in situ—Chamber techniques, *in* Hatfield, J.L., and Baker, J.M., eds., Micrometeorology in agricultural systems: Soil Science Society of America Agronomy Monograph 47, p. 247–286.

Rustad, L.E., Huntington, T.G., and Boone, R.D., 2000, Controls on soil respiration—Implications for climate change: Biogeochemistry, v. 48, p. 1–6.

State of Nevada, [1989], Well driller's report—Well log no. 32286: State of Nevada, Department of Conservation and Natural Resources, Division of Water Resources.

State of Nevada, [1994], Well driller's report—Well log no. 46918: State of Nevada, Department of Conservation and Natural Resources, Division of Water Resources.

Stevenson, I.L., 1956, Some observations on the microbial activity in re-moistened air-dried soils: Plant and Soil, v. 8, p. 170–182.

Striegl, R.G., and Armstrong, D.E., 1990, Carbon dioxide retention and carbon exchange on unsaturated Quaternary sediments: Geochimica et Cosmochimica Acta, v. 54, p. 2,277–2,283.

Swinbank, W.C., 1951, The measurement of vertical transfer of heat and water vapor by eddies in the lower atmosphere: Journal of Meteorology, v. 8, p. 135–145.

Tanner, B.D., and Greene, J.P., 1989, Measurement of sensible heat and water-vapor fluxes using eddy-correlation methods: Dugway, Utah, U.S. Army, Final report prepared for U.S. Army Dugway Proving Grounds, 17 p.

Thorstenson, D.C., Weeks, E.P., Haas, H., Busenburg, E., Plummer, L.N., and Peters, C.A., 1998, Chemistry of unsaturated zone gases at the crest of Yucca Mountain, Nevada—Data and basic concepts of chemical and physical processes in the mountain: Water Resources Research, v. 34, p. 1,507–1,529.

Turlyun, I.A., 1958, The nature of gas and vapor transfer in soil materials: Soviet Soil Science, yr. 1958, no. 9, p. 1,019–1,028.

Walvoord, M.A., Striegl, R.G., Prudic, D.E., and Stonestrom, D.A., 2005, CO_2 dynamics in the Amargosa Desert—Fluxes and isotopic speciation in a deep unsaturated zone: Water Resources Research, v. 41, W02006, 15 p.

Webb, E.K., Pearman, G.I., and Leuning, R., 1980, Correction of flux measurements for density effects due to heat and water vapour transfer: Quarterly Journal of the Royal Meteorological Society, v. 106, p. 85–100.

Publishing support provided by:
Denver Publishing Service Center, Denver, Colorado
Manuscript approved for publication March 5, 2009

For more information concerning this publication, contact:
Chief, Branch of Regional Research, Central Region
Box 25046, Mail Stop 418
Denver, CO 80225
(303) 236-5021

Or visit the USGS National Research Program Web site at:
http://water.usgs.gov/nrp/

This publication is available online at:
http://pubs.usgs.gov/sir/2009/5061/